ULTRASONIC TESTING OF ASPHALT-AGGREGATE MIXTURES

By

RICHARD WESLEY STEPHENSON

Bachelor of Science
Oklahoma State University
Stillwater, Oklahoma
1967

Master of Science
Oklahoma State University
Stillwater, Oklahoma
1968

Submitted to the Faculty of the Graduate College
of the Oklahoma State University
in partial fulfillment of the requirements
for the Degree of
DOCTOR OF PHILOSOPHY
May, 1972

ULTRASONIC TESTING OF ASPHALT-AGGREGATE MIXTURES

Thesis Approved:

Phillip L. Marker
Thesis Adviser

James V. Parker

Richard F. Lowery

L. Gilla Halibanta

N. Durham
Dean of the Graduate College

To my wife, Lonna, without whose love, faith, and sacrifice this study would have been impossible.

ACKNOWLEDGMENTS

The author could never express on paper his gratitude to his major adviser, Professor Phillip G. Manke, without whose encouragement and counsel this work would not have been completed. Dr. Manke has truly been an adviser to the author in every sense.

An expression of gratitude is necessary also to the members of the author's Graduate Committee, Professors James V. Parcher, T. A. Haliburton, and R. L. Lowery, for their encouragement and interest in this study.

The assistance of Cecil K. Sharp in preparation of special lab equipment was vital to this work.

A special thank you is given to his parents, F. W. and Hazel F. Stephenson, for instilling in the author an appreciation for the value of education.

August, 1971 R.W.S.

TABLE OF CONTENTS

Chapter		Page
I.	INTRODUCTION	1
II.	REVIEW OF LITERATURE	4
	In-Situ Testing	4
	Laboratory Testing	7
III.	THEORY AND METHOD OF ULTRASONIC MEASUREMENTS	13
	Waves in Elastic Bodies	13
	Generation and Reception of Ultrasonic Waves	19
	Acoustic Coupling	24
	Frequency	26
	Pulse Width	27
	Surface Area of Transducer	28
	Principles of Ultrasonic Measurements	30
	Flaw Detection	30
	Material Property Evaluation	34
IV.	TESTING DETAILS	39
	Equipment	39
	Electronic Equipment	39
	Temperature Monitoring Equipment	48
	Environmental Control Equipment	50
	Sample Preparation Equipment	50
	Materials	52
	Aggregate	52
	Asphalt Cement	52
	Sample Preparation	52
	Testing Procedure	53
	General	53
	Longitudinal Wave Velocity Measurements	58
	Transverse Wave Velocity Measurements	61
	Precision	66
V.	TEST RESULTS AND DISCUSSION	68
	Introduction	68
	Temperature Effects	68
	Compressional Wave Tests	69
	Shear Wave Tests	74
	Asphalt Content Effects	77

Chapter Page

V. (CONTINUED)

Void Content Effects 81
Compressional Wave Tests 81
Shear Wave Tests 83
"Elastic" Constants 84
E-Modulus 85
G-Modulus 88
Poisson's Ratio 88
Tests on Marshall Specimens 91

VI. CONCLUSIONS 93

VII. RECOMMENDATIONS FOR FURTHER RESEARCH 96

BIBLIOGRAPHY 99

APPENDIX - DERIVATION OF WAVE VELOCITY EQUATIONS 104

LIST OF TABLES

Table		Page
I.	Piezoelectric Transducer Constants	25
II.	Specifications of Gulton HST-41 Ceramic	43
III.	Comparison of Shear Wave Velocity Measurements	65

LIST OF FIGURES

Figure		Page
1.	Particle Displacement of Longitudinal and Transverse Waves	14
2.	Wave Reflection at a Free Surface	17
3.	Wave Reflection and Refraction at a Plane Interface	17
4.	Schematic Diagram of Quartz Crystal	21
5.	Schematic Diagram of X-Cut Quartz Plate	21
6.	Schematic Diagram of Quartz Lattice	22
7.	Schematic Diagram of Deformed Quartz Lattice	22
8.	Approximate Shape of Ultrasonic Beam for Large Values of $2a/\lambda$	29
9.	Schematic Diagram of Pulse Echo Technique	29
10.	Shadow (Transmission) Method	32
11.	Interference Method	32
12.	Testing Apparatus	40
13.	Trace of Source Pulse	40
14.	Schematic Wiring Diagram of Pulse Generator	42
15.	Compressional Wave Crystals	44
16.	Holding Device With Specimen in Place	44
17.	Shear Wave Crystals	45
18.	Time Measurement on Oscilloscope Using Delayed Sweep	47
19.	Thermistor	49
20.	Temperature Monitoring Apparatus With Sample Specimen	51
21.	Motorized Gyratory-Shear Compactor	51

Figure Page

22. Combined Aggregate Grading Chart 54

23. Schematic Diagram of Ultrasonic Wave Paths and the Trace Indication of Their Reception 57

24. Schematic Diagram Showing Reflection of Waves in Test Medium and Schematic Scope Trace 59

25. Oscilloscope Trace of Longitudinal Wave Through 4% Asphalt Concrete 60

26. Oscilloscope Trace of Transverse Wave Through 6% Asphalt Concrete 63

27. Schematic Diagram of Equipment Components and Test Arrangement 67

28. Effect of Temperature on Longitudinal Wave in 4% Asphalt Concrete 70

29. Compressional Wave Velocity Versus Temperature 71

30. Effect of Temperature on the Transverse Wave in 6% Asphalt Concrete 75

31. Shear Wave Velocity Versus Temperature 76

32. Effect of Per Cent Asphalt Content on Compressional Wave Velocity 78

33. Effect of Per Cent Asphalt Content on Shear Wave Velocity 79

34. Effect of Per Cent Void Content on Ultrasonic Wave Velocity 82

35. E-Modulus Versus Temperature 86

36. G-Modulus Versus Temperature 89

37. Poisson's Ratio Versus Temperature 90

38. Stresses Acting in X-Direction on a Small Rectangular Parallelepiped 105

CHAPTER I

INTRODUCTION

Most procedures in use today for the design of flexible pavement systems employ empirical techniques that have proven adequate over the years. There are almost as many design procedures as there are agencies using them. Among the more widely used methods are the California Bearing Ratio Method, the North Dakota Cone Method, the Group Index Method, the Corps of Engineers Method, and the Asphalt Institute Method.

In an effort to standardize design techniques, much attention has been and is being focused on procedures that treat the pavement system as a structural assembly. Impetus in this direction was fueled by the American Association of State Highway Officials (AASHO) Road Test. Another important factor influencing this effort was the instigation of the International Conference on the Structural Design of Asphalt Pavements which convened first in 1962 and again in 1967 at the University of Michigan.

In treating asphalt pavements as though they consisted of structural components, the major obstacle to overcome is that of determining the parameters defining the material's behavior under load. Although it is recognized that the system is not elastic, elastic theory has been utilized. Strength parameters, such as the modulus of deformation taken from the stress-strain curve of a confined compression test, have been

used in design. The California Bearing Ratio, determined from relating the penetration of a standard plunger into the test material to that of the penetration in a standard crushed rock material, is also a widely used strength parameter.

One problem with using these methods to determine material constants lies in the fact that the tests involve static loading conditions while an in-situ pavement is subjected primarily to dynamic loading. Another problem arises due to the destructive nature of the tests. Once a laboratory specimen has been tested by this method, it is no longer usable. This, coupled with the gross inhomogeneity of the material under study, introduces a large degree of variation from test sample to test sample.

A testing method for road construction materials is needed which permits the determination of material constants from evaluative procedures that more closely approximate the type of loading and the loading conditions existing under actual use. This test should be such that a single material sample could be tested many times under varying conditions using a repetitive or dynamic loading technique. That is, a nondestructive, dynamic test procedure is desired.

In this study, a test technique used by acoustic engineers in their study of more homogeneous materials such as metals, plastics, ceramics, and glass has been applied to asphaltic paving materials. By measuring the propagation velocity of high frequency sound waves through the material, various material constants can be determined. The advantages of this technique are primarily threefold. First, the test procedure is nondestructive, permitting many measurements to be made on the same specimen. Secondly, the test procedure is dynamic, and more closely

approaches the type of loading occurring on the in-situ structure. Thirdly, the test is easily and rapidly performed.

While this testing technique has certain advantages over standard types of tests and shows great promise of becoming a valuable tool for the engineer for design and analysis of flexible paving materials, it is not a testing panacea at the present stage of development. The electronic equipment required for this technique is expensive. In addition, the operator of the equipment should possess some knowledge of the expected behavior of the material under test as well as a working knowledge of acoustical theory. Another drawback is one common with other dynamic methods of testing asphalt concrete, i.e., the assumption that elastic theory holds true for this material.

The primary objective of this work was to develop instrumentation by which the propagation velocity of both the shear and compressional waves could be directly determined. In support of this development, the relationship between the respective wave velocities and material temperatures over a temperature range representative of in-service conditions were to be determined. The effects of asphalt content and/or void content upon the acoustic wave velocities in a specific mixture were examined. Another area of interest was to be the determination of the material constants determined from eleastic theory equations, i.e., E-modulus, G-modulus, and Poisson's ratio, and their variation with temperature.

CHAPTER II

REVIEW OF LITERATURE

In recent years, nondestructive dynamic testing of pavement materials has been emerging from the shadows of speculative research to take its place as a useful tool for the practicing highway engineer. The illogical use of static tests to design structures which, in reality, operate under dynamic loading conditions has long been questioned by many engineers.

In essence, the goal of dynamic testing of roadway materials has been to evaluate the primary elastic properties (Young's modulus, E, and the shear modulus, G) of the materials for their dynamic behavioral characteristics. From these values, various theories give the possibility of calculating stress and deflection in the pavement system.

Since the late 1930's, dynamic testing of roads and road construction materials has developed along two lines. The first has been the study of pavement systems in-situ. The second concerns the study of the individual pavement materials in a laboratory environment.

In-Situ Testing

As early as 1928, German research engineers were utilizing nondestructive vibrational techniques to study the response characteristics

of roads and runways (12) (7) (41).[1] Elastic waves generated on in-situ pavements by a mechanical oscillator of the rotary out-of-balance type were analyzed to determine vibrational behavior.

Perhaps the leader in field testing of pavement systems has been the Amsterdam Koninklijke/Shell-Laboratorium (13). The Shell laboratory developed a heavy mechanical vibrator along the same lines as Deutsches Gesellschaft fur Bodenmechanik (DEGEBO). The Shell vibrator is capable of generating alternating vertical forces of a few tons corresponding in magnitude and frequency to the forces exerted on pavements by heavy trucks. This vibrator, developed by van der Poel (50), allows measurement of dynamic deflections and also generates a stress wave of sufficient power to penetrate up to 10 meters of pavement depth. Nijboer (37) developed a light electrodynamic vibrator for higher frequency waves with lower penetrating power. All the equipment is mobile and self-contained.

Initial tests with this equipment were carried out in three phases (15). First, tests on subgrades established several points of interest. It was found that a rough correlation between the dynamic modulus of elasticity computed from observations of the wave velocity (V) and the true density (d) of the medium through which the waves are propagated ($E \propto dV^2$) and field CBR values seemed to exist, i.e., $E \simeq 100$ CBR. It was also determined that E decreased with increasing water content (in clay), while increasing with increasing compactive effort. Compacted unbound granular material placed to serve as subbases was found to have an upper limit for the E modulus which was no greater than the E modulus

---

[1]The numbers in parentheses correspond to the listing of the reference in the Bibliography.

of the underlying soil.

Tests on unbound base course materials revealed that their E values were dependent on the rigidity of the underlying material. Bound materials, on the other hand, exhibited much higher E values which were only slightly effected by the properties of the subgrade material. Bituminous base courses as well as surface courses had approximately the same E values. This E value was highly dependent upon temperature. Base courses constructed with lean Portland cement had properties which were independent of temperature.

Finally, tests were run on the complete pavement system. It was found that these tests could be used to evaluate the condition of the pavement system at considerable depth as well as to provide a means of following progressive alteration in the pavement properties with time (14).

Another apparatus for in-situ testing employed by E. N. Thrower (48), at the Road Research Laboratory in England, also provided dynamic loading for pavement structures. Thrower's tests demonstrated that the dynamic elastic moduli for bituminous materials were both frequency and temperature dependent and were complex in character. An increase of modulus values corresponded both to an increase in test frequency and a decrease in material temperature.

The Road Research Laboratory (52) has developed test apparatus for measuring moduli of soils specifically applicable to pavement design. An axial load is applied to a triaxial sample by means of a cam and a spring imparting a realistic form of stress pulse to the sample. Lateral pressure on the sample can also be applied in phase with the axial loading. From these tests, the dynamic modulus of elasticity for

soil types usually found under roads appeared to range from 3000 to 60,000 psi.

Recently, a new two degree-of-freedom vibrator has been proposed as a testing apparatus for in-situ materials (51). The two degree-of-freedom system has the advantage of operating throughout the entire frequency range of interest as well as allowing a significant reduction in the weight of the apparatus itself.

C. T. Metcalf (34) has developed a high frequency vibrator centering around a Goodman electromagnetic vibrator capable of exerting forces upon in-situ materials of up to 15 kilograms. Using this equipment, Metcalf tested pavement structures at test sites located in Colorado and in Minnesota. He concluded that temperature significantly influenced wave velocity and that the type of material incorporated in the pavement structure effected the stress wave velocities.

Recently, Michael E. Szendrei and Charles R. Freeme (47) have published reports of vibrational testing procedures by which wave propagation, attenuation, and impedence measurements on in-place road pavements were combined to evaluate deflections under a moving load.

Laboratory Testing

At the present time, laboratory testing of materials provides the most advanced and most sophisticated means of evaluating material properties. The advantages of being able to isolate the material variables under study from extraneous interfering influences as well as the advantage of being able to closely control sample preparation and the atmospheric environment allow the observation of behavioral characteristics which are often not measurable by field testing methods.

Laboratory dynamic tests are usually conducted on the individual pavement constitutents, i.e., subgrade materials (clay), subbase (sand and gravel), base course (stabilized material), and surface course (asphalt concrete or Portland cement concrete). The two major types of laboratory dynamic tests usually applied to soils are variations on dynamic triaxial tests, and stress wave propagation analyses.

Kenneth L. Lee and H. Bolton Seed (27) developed a test procedure in which a triaxial specimen was subjected to pulsating cyclic loadings. They concluded that the strength of the specimen under pulsating loading conditions was found to increase with increasing density, increasing confining pressure, and increasing ratio of major to minor principal stress under consolidation. They also found that a comparison of the pulsating loading strength with the static strengths for the three soils (2 sands and a compacted silt) investigated failed to suggest any unique relationship which might be used to predict the pulsating loading strength from the results of static loading tests.

The dynamic modulus of elasticity of sand and the effect of stress condition on the modulus were studied by Shannon, Yamane, and Dietrich (44) using a test apparatus similar to a triaxial compression apparatus. The base of the specimen was secured to a diaphragm which could be forced to vibrate at small amplitude by an externally applied vibrator. The results indicated an increase in modulus with confining pressure and an increase in the resonant frequency of the sample with confining pressure as well.

In one experimental study, over two hundred tests were performed on samples representing three basic soil types to study the relationship between pulse velocity, dry density, water content, and compactive

effort. The wave velocities were determined using a James Electronics, Inc. V-Scope (45). It was found that pulse velocity increased monotonically with dry density for a constant water content until a maximum velocity was reached after which velocity decreased with increasing dry density.

Brown and Pell (3) studied the behavior of a clay of medium plasticity when subjected to a dynamic load pulse. Their measurements of stress and strain distribution indicated that the stresses generally agreed well with Boussinesq Theory. Loyd D. Hampton (11) measured the acoustic properties of sediments using pulse techniques. He defined relationships for the frequency dependence of attenuation of the sediments.

The dynamic characteristics of surfacing materials have been studied by several test methods. Flexure tests on Portland cement concrete and asphalt concrete have been carried out by many investigators. Monismith (35) employed a test system in which an apparatus consisting of a spring base to simulate the base-subgrade combination in the field and a device to apply repeated loadings of short duration was used to test flexure properties. He found that the fatigue resistance of a paving mixture increased with asphalt content and that there was little influence due to differing physical properties of the incorporated asphalt binder. Monismith also determined that the deformation induced in a paving mixture was a better criterion for determining the behavior of a paving mixture in repeated flexure than deflection alone.

Jimenez and Gallaway (19) studied the resistance to repetitive loading of slab-type asphalt concrete specimens both laboratory-fabricated and cut from existing roads. They utilized a "deflectometer"

which supplied vertical loading by the rotation of two eccentrics. The specimen was clamped and supported by a rubber membrane which was in turn supported by oil pressure. They concluded from their tests two principal facts. First, the flexibility of thin asphaltic concrete slabs is greater than that of thicker ones but the thinner slabs have less resistance to repeated load. Second, they determined that an increase in the support given a slab of asphaltic concrete will increase its resistance to repeated loads, but may decrease the amount of tolerable deflection of the slab.

Papazian (39) foresees the development and adaption of viscoelastic methods of pavement analysis and design as does Pagen (38) and Krokosky (26). Papazian subjected cylindrical test specimens of dense-graded asphaltic concrete to sinusoidal-stress dynamic tests and constant stress static tests, yielding values of the complex elastic modulus, E*, and the complex transverse modulus, T*. The dynamic tests indicated that asphaltic concrete is a reasonably linear material having well defined complex moduli whose magnitude and phase vary with frequency.

Chen and Hennes (5) combined vibrosonic tests and flexural tests to define a "dynamic modulus of rupture" for asphaltic concrete. Vibrosonic tests make use of the relationship which exists between the resonant frequency of the test specimen and its size, density, and modulus of elasticity. Vibrosonic test techniques were also utilized by Goetz (9) to calculate modulus of elasticity values from resonant frequency measurements. He concluded that even though the modulus of elasticity values calculated using elastic theory may not be strictly valid (particularly at temperatures greater than 40°F) such measurements do provide valuable information concerning the elastic-plastic

characteristics of bituminous-aggregate mixtures.

Pulse velocity testing techniques utilizing ultrasonic waves have been accepted as important testing tools for the engineer. These methods are used to locate defects in metallic and non-metallic materials and to examine the structure of the material to ascertain its dimensions as well as its physical properties. The advantage of this method of testing is the nondependence upon specimen configuration and the ease and speed by which the test can be performed.

Although it has been determined that changes in pulse velocity or dynamic modulus in a particular specimen of structural concrete are related to its strength properties, there seems to be no evidence that a unique relationship between pulse velocity and strength exists (2). Further tests on concrete were done by both Whitehurst (53) and Parker (40). Both investigators arrived at similar conclusions:

1. The absence of internal cracking in concrete is indicated by pulse transmission through the mass at normal velocity; the presence of such cracks would be suggested by absence of a received signal or abnormal delay in its arrival.
2. The depth of surface cracks may be ascertained.
3. Compressive strength can only be approximated even with known materials.

Manke and Gallaway (32) investigated pulse velocities in flexible pavement construction materials. They found that the pulse velocities in clays and more granular highway construction materials were related to moisture content, density, confining pressure, and cementitious material in the voids. In bituminous mixtures, they found that the characteristics of the asphalt binder influenced the wave propagation.

They concluded that velocity increases with increasing asphalt content up to an expected limiting content for a given aggregate mixture and that velocity decreases with increasing temperature and increases with increasing density. They also suggested that pulse techniques using both shear and compressional wave forms could provide a useful method of determining the elastic constants of flexible pavement materials.

Previous work in ultransonic compressional wave testing done at Oklahoma State University has attempted to delineate the elastic, "elasto-plastic", and plastic behavioral temperature ranges of asphalt aggregate mixtures (46). It was found that temperature did indeed significantly influence compressional wave velocities in the asphalt concrete. Other influencing factors were asphalt content and asphalt consistency. It was also shown that Poisson's ratio has an appreciable influence on pulse modulus values and, therefore, should not be assumed for accurate evaluation of the elastic properties of the mixture.

CHAPTER III

THEORY AND METHOD OF ULTRASONIC MEASUREMENTS

Waves in Elastic Bodies

There are two general types of waves that can be propagated in an extended elastic medium; longitudinal and transverse. These wave types are so named in regard to the particle displacement relative to the direction of propagation of the wave. As shown in Figure 1, the direction of propagation of a longitudinal (compressional) wave is parallel to the axis of particle displacement. For transverse (shear) wave forms, the direction of propagation is transverse to the particle displacement. Longitudinal waves can be propagated in media which have volume elasticity, i.e., all types of media. Transverse waves are only propagated in media which has shear elasticity, i.e., solids only.

Another type of wave, whose particles move in both the longitudinal and transverse directions, is propagated, if the solid medium is bounded by a free surface. This wave form, known as a surface or Rayleigh wave (after Lord Rayleigh), is propagated along the surface of the medium. Its intensity diminishes rapidly in the direction perpendicular to the plane of the surface. At a depth of 1.5 times the wavelength (λ), the intensity (I) is approximately equal to zero (8). The velocity of transmission of the various wave forms is a function of the density and the elastic constants of the medium.

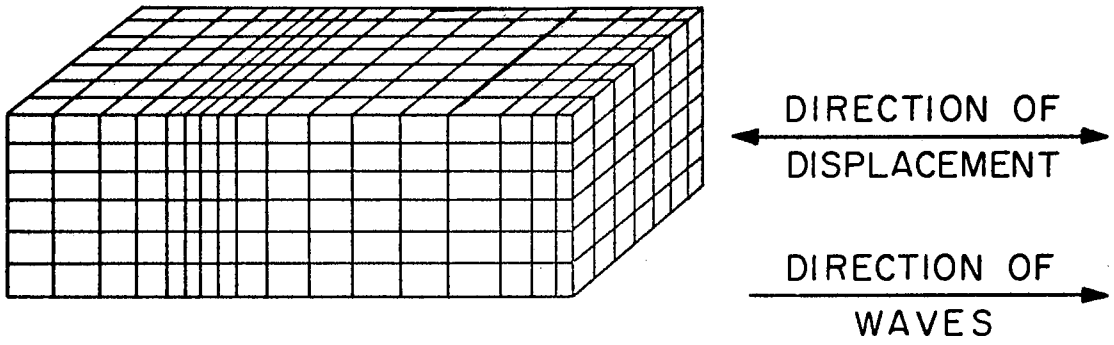

Longitudinal Waves

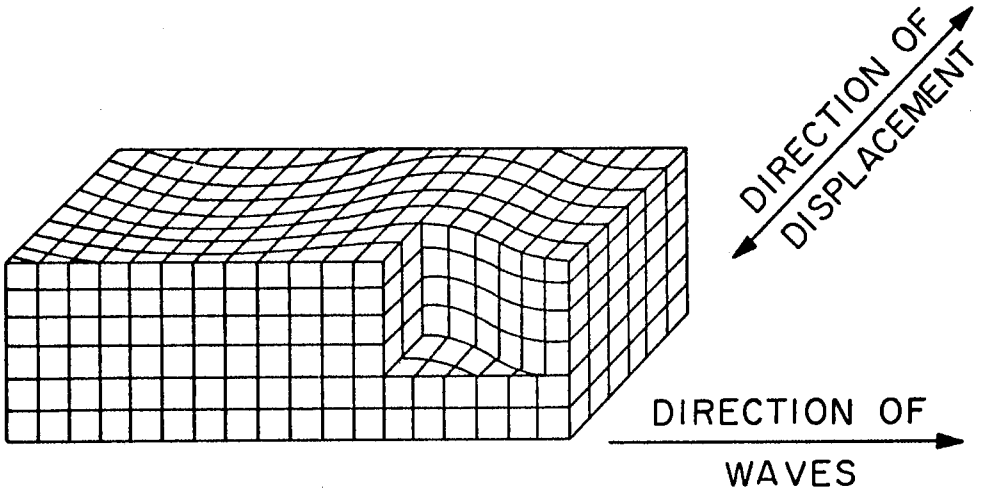

Transverse Waves

Figure 1. Particle Displacement of Longitudinal and Transverse Waves

From elastic theory (see Appendix A), it can be shown that:

$$V_c = \sqrt{\frac{E(1-\nu)}{\rho(1+\nu)(1-2\nu)}} \tag{1}$$

and

$$V_s = \sqrt{\frac{E}{2\rho(1+\nu)}} \tag{2}$$

where:

V_c = Velocity of the compressional wave

V_s = Velocity of the shear wave

ν = Poisson's ratio

E = Young's modulus

ρ = Mass density = $\frac{\gamma}{g}$

γ = Bulk density

g = Acceleration due to gravity.

From Equations (1) and (2), the relationship for Poisson's ratio can be expressed as:

$$\nu = \frac{1 - \frac{1}{2}(V_c/V_s)^2}{1 + (V_c/V_s)^2} . \tag{3}$$

From these equations, it is seen that by measuring the velocity of both the shear and compressional waves in a single test specimen, Poisson's ratio, Young's modulus, and even the shear modulus of that specimen can be computed.

The measurement of these quantities is complicated by a phenomenon known as mode conversion. Mode conversion occurs when a wave of one type is transformed into a wave of a different type.

When a single shear or compressional wave, traveling in a test

medium, strikes a free surface, two reflected waves are generated (Figure 2). A wave (A_2) of the same type as the incident wave (A_1) is reflected at an angle equal to the angle of incidence. A wave (A_3) of the other type is also generated whose direction of travel is at an angle β. α and β are related by the equation:

$$\frac{\text{Sin } \alpha}{\text{Sin } \beta} = \frac{V_1}{V_2}$$

where:

V_1 = Velocity of propagation of the incident wave.

V_2 = Velocity of propagation of the generated wave.

The acoustic impedence of a material (W) is defined as the product of the material density and the velocity of sound in that medium ($W = \rho c$). Materials with high sound resistance (impedence) are called "sonically hard", while those with low sound resistance are known as "sonically soft". Sound wave pressure (P), intensity (I) and acoustic impedence are related through the following relationships:

$$P = W \omega A$$

$$I = \frac{\frac{1}{2}P^2}{W}$$

where:

ω = Angular frequency of sound wave.

A = Amplitude of particle motion.

When either a compressional or a shear wave, traveling through a solid medium, impinges on a boundary between two media both reflection and refraction occur. Four separate waves are generated: shear and compressional waves are reflected and shear and compressional waves are

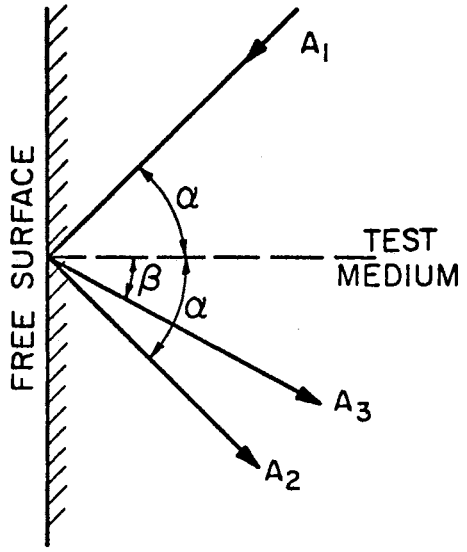

Figure 2. Wave Reflection at a Free Surface

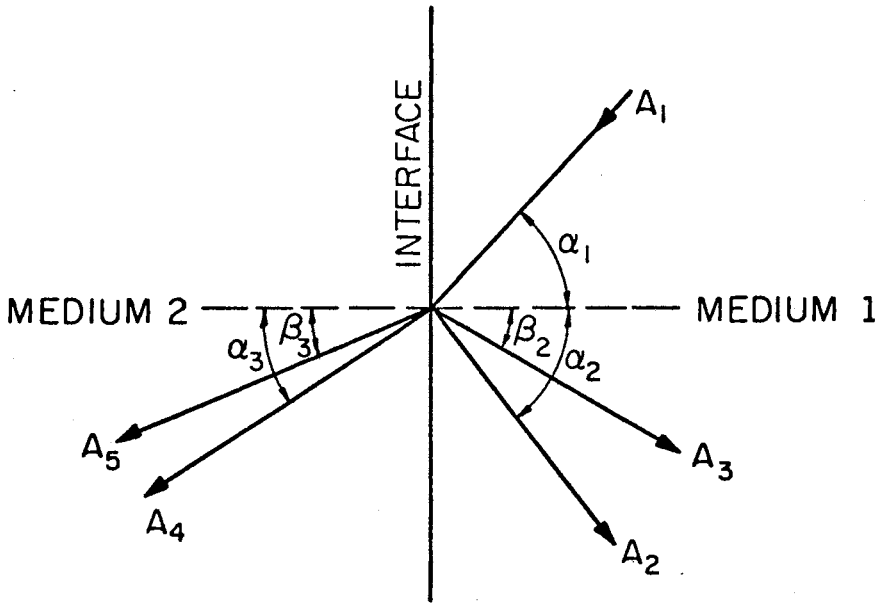

Figure 3. Wave Reflection and Refraction at a Plane Interface

refracted (Figure 3). The governing equation of this case is:

$$\frac{\text{Sin } \alpha_1}{V_{c1}} = \frac{\text{Sin } \alpha_2}{V_{c1}} = \frac{\text{Sin } \beta_2}{V_{s1}} = \frac{\text{Sin } \alpha_3}{V_{c2}} = \frac{\text{Sin } \beta_3}{V_{s2}} \qquad (5)$$

where:

V_{c1} = Compressional wave velocity, material 1.

V_{c2} = Compressional wave velocity, material 2.

V_{s1} = Shear wave velocity, material 1.

V_{s2} = Shear wave velocity, material 2.

The reduction in intensity of an ultrasonic wave is called attenuation. In a solid material, there are two general methods by which attenuation occurs; absorption and scattering. Scattering results from the fact that the material under test is neither extended nor strictly homogeneous. In a non-homogeneous material, there are boundaries at which the acoustic impedance changes abruptly because two materials of different density or sound velocities meet at these interfaces. On an oblique boundary, the wave is split into various reflected and transmitted wave types; i.e., reflection and refraction occurs at this boundary. This process repeats itself for each wave at the next boundary. Thus, the original sound wave is continually separated into different waves which, along their complex paths through the material, are gradually converted into heat.

Absorption is a direct conversion of sound energy into heat. Several processes for this energy conversion may be responsible (24). The processes involved are beyond the scope of this study. However, absorption can be roughly visualized as a sort of braking effect on the oscillation of the particles. This visualization also helps to explain

why a rapid oscillation loses more energy than a slow oscillation; i.e., the absorption usually increases with the frequency of oscillation (25).

Both types of losses limit the ultrasonic testing of materials. Pure absorption reduces the transmitted energy. This can be overcome by increasing the input wave energy and the output amplification. Scattering not only reduces the energy levels, but also produces different waves with different transit times in which the true wave may get lost.

Generation and Reception of Ultrasonic Waves

Ultrasonic waves are sound waves that have a frequency greater than that discernible by the human ear (>15-20 kc). The introduction of ultrasonic waves into a material is accomplished by placing the material in contact with a vibrator which oscillates with the desired wave form and frequency. The generated waves are detected in a similar manner by placing the material in contact with a receiver which is capable of measuring the sound pressure of an incident wave. The most efficient and most widely used method of generation and reception of ultrasound has been the utilization of the physical phenomenon known as the piezoelectric effect.

Piezoelectricity is "pressure electricity". It was discovered by Pierre and Jacques Curie in the 1880's. When a piezoelectric material is deformed by external mechanical pressure, electric charges are produced on its surface. The reverse phenomenon occurs when such a material is placed between two electrodes. The material changes its form if an electric potential is applied across the elctrodes. This is known as the inverse piezoelectric effect. The primary effect is used for reception of ultrasonic waves and the inverse effect is used for the

generation of ultrasonic waves.

The piezoelectric effect is a property of the crystal structure and is linked to an assymetry in it which can be characterized by the appearance of one or several polar axes (dipoles). A dipole results from a difference between the average location of the positive charges and the average location of the negative charges in a molecule.

In the case of quartz, a common piezoelectric material which occurs in nature in the form of hexagonal prisms, there are three polar axis, X_1, X_2, and X_3 each of which passes through two opposite edges of the crystal (Figure 4). The Z-axis of the crystal is parallel to the axis of the prism and is also called the optical axis. In addition, there are three Y axes normal to the Z axes and the X axes; i.e., they pass through the centers of two opposite sides of the hexagon.

The piezoelectric effect is best analyzed by using plates cut from the quartz crystal at right angles to an X-axis (X-cut) (Figure 5). A schematic of the crystal lattice structure itself is shown in Figure 6.

Any pressure on the X-cut quartz plate slightly reduces its thickness because it is elastic. This shifts the electrically charged elements of the crystal lattice in a way relative to each other such that the plate becomes polarized. As a result, free positive charges appear on one side of the plate and negative charges on the other (Figure 7). For convenient discharge of the electric potential, metal electrodes are used that are firmly attached to both sides of the plate. These layers form an electric capacitor with the crystal as the dielectric. The X-cut quartz is used to generate longitudinal waves in a solid.

A Y-cut quartz plate is cut from the quartz crystal at right angles to a Y-axis. The Y-cut crystal deforms in plane upon application of an

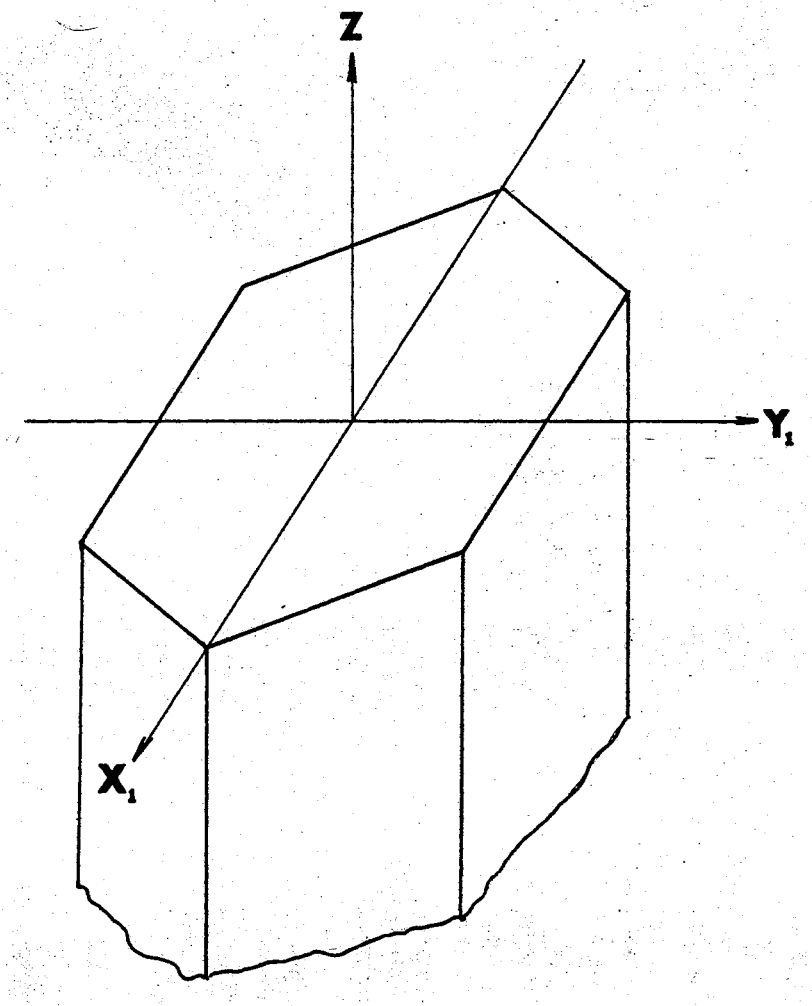

Figure 4. Schematic Diagram of Quartz Crystal

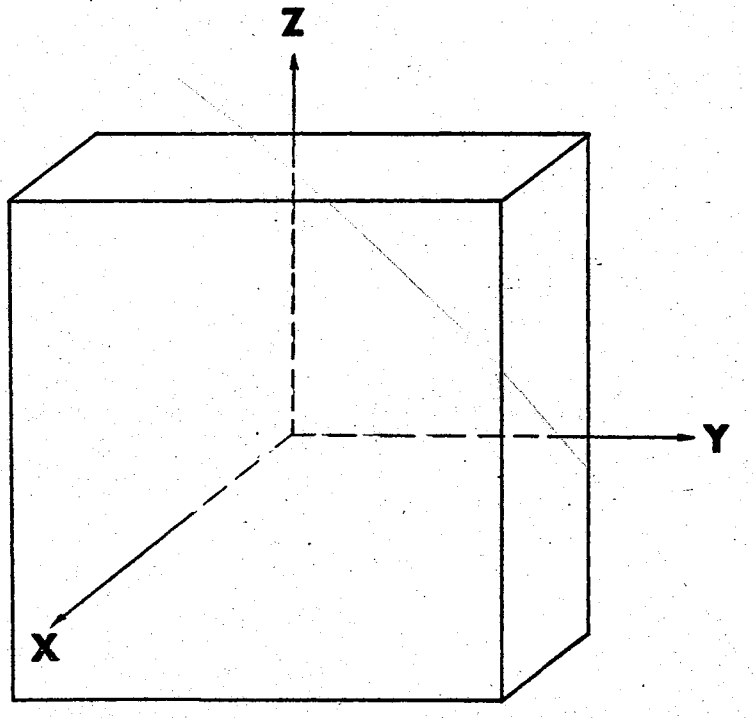

Figure 5. Schematic Diagram of X-Cut Quartz Plate

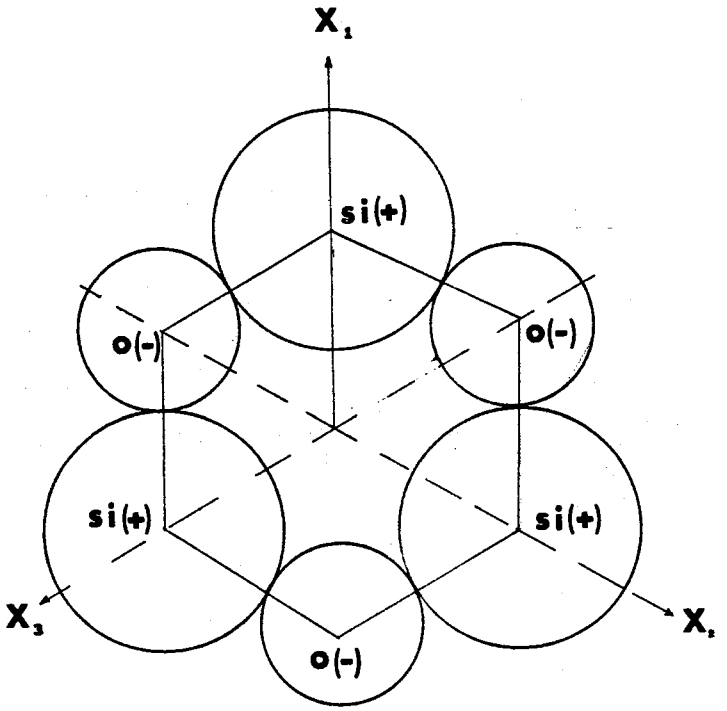

Figure 6. Schematic Diagram of Quartz Lattice

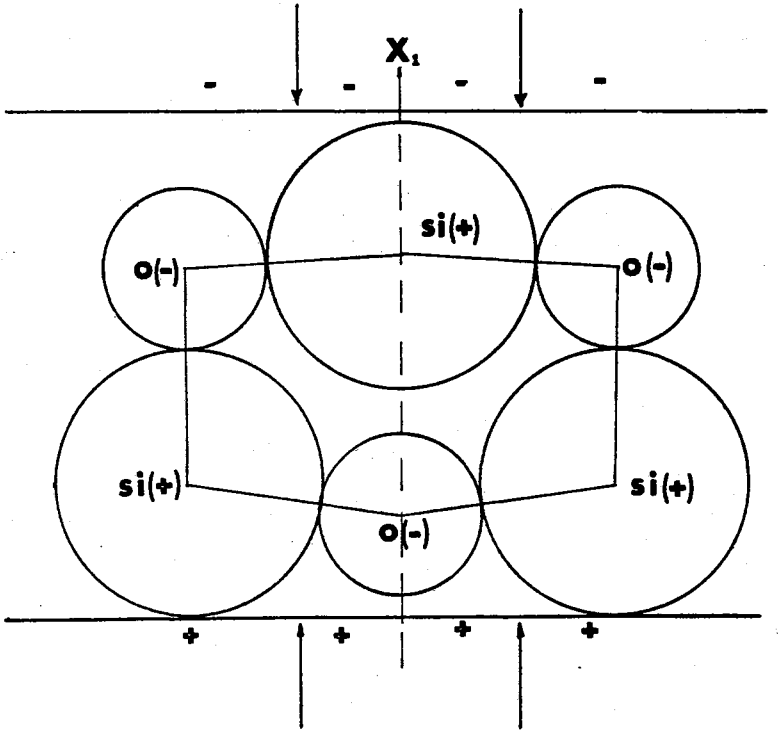

Figure 7. Schematic Diagram of Deformed Quartz Lattice

electric charge. This crystal is used to generate transverse waves in a solid.

Piezoelectric materials are manufactured from ceramics. A ceramic is composed of a multitude of crystals in random orientation. Its properties are the sum of the properties of all these crystallites. Such a ceramic can be poled by a strong d.c. field. It will then behave roughly like a single domain ferroelectric crystal and will be piezoelectric.

One of the most significant features of piezoelectric ceramics is their great stiffness. The deflections in response to a driving signal are very small, but they are very strong and not easily blocked. Piezoelectric ceramics are also very sensitive to small deflections and, therefore, serve very well as ultrasonic pickups.

The best measure of the ability of a piezoelectric to act as a transducer of energy is the electromechanical coupling coefficient, k. The square of the coupling coefficient is the fraction of the input energy of one kind stored in the ceramic as energy of the second kind:

$$k^2 = \frac{\text{mechanical energy converted to electric charge}}{\text{input mechanical energy}} .$$

The dielectric constant (K_i) measures the amount of charge that an electroded slab of material can store, relative to the charge that would be stored by identical electrodes separated by air or vacuum at the same voltage.

The piezoelectric charge coefficients, d, are the ratios of the electric charge generated per unit area to the force applied per unit area. These constants are generally written as tensor components with

subscripts d_{ij}. The first subscript is the electrical direction, the second is the mechanical direction.

The g_{ij} coefficients are the ratio of the electric field produced to the applied mechanical stress:

$$g = \frac{\text{volts/meter}}{\text{newtons/square meter}}.$$

The g and d coefficients are related to each other by the dielectric constant, K_i, as, in a capacitor, the voltage V is related to the charge Q by the capacitance C. The equations are:

$$Q = CV$$

$$d_{33} = K_3 \epsilon_0 g_{33}$$

$$d_{31} = K_3 \epsilon_0 g_{31}$$

$$d_{15} = K_1 \epsilon_0 g_{15}.$$

ϵ_0 is the absolute dielectric constant equal to 8.85×10^{-12} farads per meter. Typical values of the constants described above are given in Table I for several of the most widely used piezoelectric transducers.

Acoustic Coupling

Many of the limitations of ultrasonic testing arise from the method of contact between the transducer and the surface of the test specimen, i.e., the degree of acoustic coupling. The degree of coupling depends upon the surface roughness of the material under test and the nature of the couplant material itself. In general, the smoother the surface of the specimen the better the coupling between the surface and the transducer and the better the penetration of ultrasound into the test

TABLE I

PIEZOELECTRIC TRANSDUCER CONSTANTS

	Dielectric Constant	Electromechanical Coupling Coefficient		Piezoelectric Charge Coefficient	Piezoelectric Pressure Constant
	ϵ	k_{33}	k_{15}	d_{33} (10^{-12}m/v)	g_{33} (10^{-3}V/m)
Quartz	4.5	0.10	0.10	2.3	57
Lithium Sulfate	10.3	0.35	0.0	15	165
Barium Titanate	1700	0.52	0.37	190	11
Lead Metaniobate	225	0.42	0.07	80	37
Lead Zirconate Titanate	1800	0.66	0.69	325	22

specimen. As surface roughness increases, lower frequencies must be used to insure that sufficient energy is transmitted to the test material and to reduce scattering at the surface.

The difficulty in choosing the couplant material is again the problem of impedance match. Since the sonic wave passes from the transducer into the couplant material and then from the couplant into the test material, the impedance match between both interfaces must be at an optimum.

By far, the most widely used couplant is oil; usually oil of low viscosity. A non-dripping grease (silicone grease) is used in many cases as well. Highly viscous materials, such as mixtures of wax and oil and vegetable resins can be used for coupling normal probes for transverse waves. On smooth and flat surfaces, it is more practical to press the dry transducer against the specimen using a clamping device or weight. The probe can also be stuck on the specimen using an adhesive agent.

Intermediate layers are sometimes used to protect the transducer from wear. This procedure, of course, broadens the pulse and a couplant is still required between the probe and the test material.

Frequency

The frequency (f), wavelength (λ), and sonic velocity (v) are interrelated by the well-known equation: $v = f\lambda$. Since the sonic velocity of any material is ideally constant, it is easy to see that the frequency is proportional to the inverse of the wavelength. Increasing the frequency decreases the wavelength of the ultrasonic beam in the material. This, in turn, causes a greater concentration of the beam

and, therefore, a higher wave intensity. A higher wave intensity generates an increase in the voltage at the electrodes of the receiving transducer. Hence, an increase in frequency gives rise to an increase in sensitivity. On the other hand, a decrease in the wavelength increases the absorption of the wave. It is, therefore, advantageous to use as high a frequency as possible consistent with tolerable absorption.

Pulse Width

When an electrical signal is applied to the electrodes of a piezoelectric transducer, the transducer begins vibrating with increasing amplitude until a condition of steady-state is reached. Similarly, when the excitation voltage is removed, the oscillation amplitude of the transducer decreases to zero in an exponential manner. If the applied electrical signal has a frequency equal to the resonant frequency of the transducer, the transducer will oscillate at its maximum amplitude. However, if the applied electrical frequency is different than the resonant frequency of the crystal, the transducer will oscillate not only at its resonant frequency, but also at its harmonics. When the applied voltage is removed, the transducer does not cease vibration immediately. The amplitude of oscillation decreases as a function of the damping factor δ.

The effects of pulse width are most important when ultrasonics are used for flaw detection. When an electrical pulse is applied to a transducer, the oscillations build up gradually to a steady-state condition of maximum amplitude in a finite period of time. If the electrical pulse is too narrow for the vibration of the transducer to reach

resonance, the wave amplitude in the test medium will never reach its maximum value. Therefore, for maximum detectability, the applied pulse must be wide enough to allow the transducer to resonate. However, as pulse width increases, it becomes more difficult to differentiate between two separate defects lying close together. If the distance of separation is less than the pulse width, an indication of only one flaw will be obtained.

Another drawback of broad electrical pulses is the fact that wave arrivals at the receiver are sometimes masked by secondary waves input into the specimen during the transient decay of the source transducer oscillation after the cessation of the electrical pulse. Therefore, it can be said that an increase in pulse width increases the amplitude of the input wave. Also, as the pulse width increases, there will be a corresponding loss in detectability and resolvability at the receiver.

Surface Area of Transducer

The amount of energy arriving at the receiving crystal is associated with the angle of divergence of the input beam. The less divergence, the greater the wave energy at the receiver. As shown in Figure 8, the angle of divergence of the beam, α, is given by the equation:

$$\text{Sin } 2\alpha = 0.5\ \lambda/a$$

where:

λ = wavelength

a = radius of source transducer.

If the beam hits the side of the test sample at varying low angles of incidence, it can be reflected in such a way as to return to the center

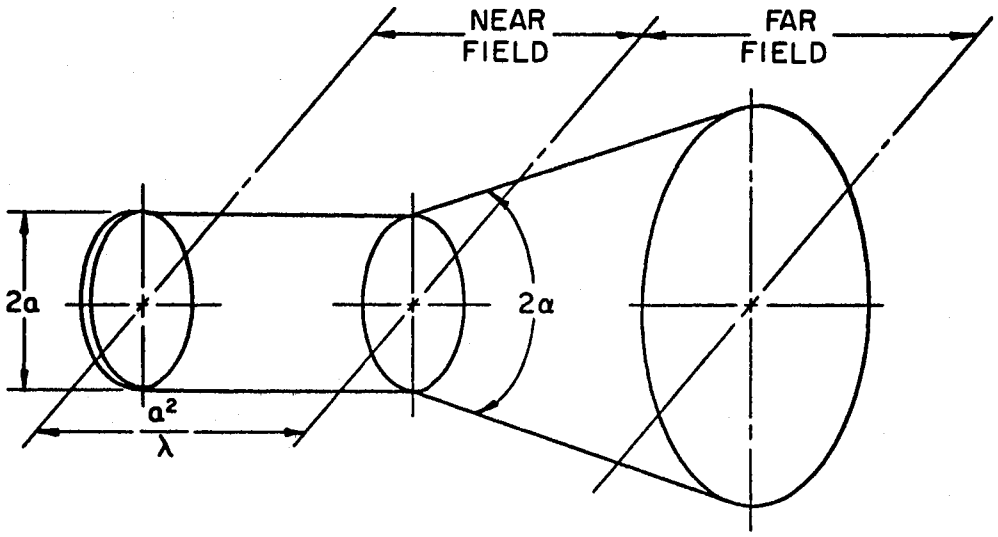

Figure 8. Approximate Shape of Ultrasonic Beam for Large Values of $2a/\lambda$

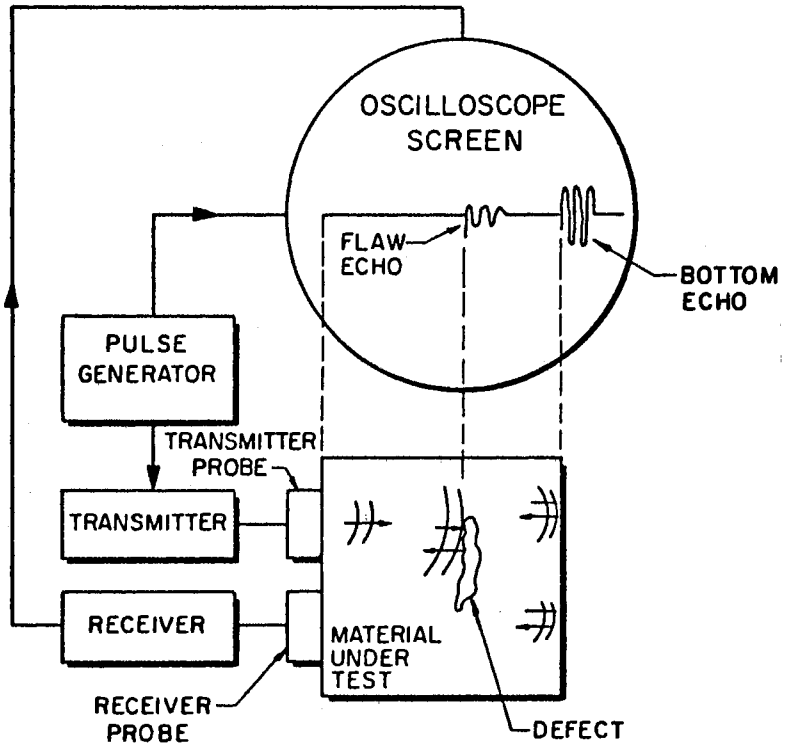

Figure 9. Schematic Diagram of Pulse Echo Technique

of the specimen after a number of reflections. The receiver can then pick up those signals which have taken a longer path than those in the part of the beam which has remained in the central section of the sample. The result of this is to have interference occur among the pulses. This phenomenon is known as the "sidewall effect". It is usually desirable to have the diameter of the specimen several times greater than that of the transducer in order to reduce sidewall effects. However, larger transducers increase the difficulties in obtaining good coupling between the crystal and the test material.

Principles of Ultrasonic Measurements

The propagation of sound waves in a medium is a function of both the elastic properties of that medium as well as the homogeneity of its structure. Ultrasonic testing procedures have been widely employed in primarily two areas: that of detecting and locating material discontinuities and for the evaluation of material elastic constants.

Flaw Detection

In flaw detection investigations, material discontinuities either reflect the waves or provide a shadow of them. The testing techniques fall primarily into three categories: the echo method, the shadow method, and the resonance method.

The Echo Method. A given flaw in a test medium presents an obstacle to the propagation of an induced sound wave. Since the flaw represents the inclusion of a material having an acoustic impedance differing from that of the surrounding test medium, the sound waves are at least partially reflected when they impinge on the test material/flaw

interface (Figure 9). A measurement of the time between the input of the original wave and the arrival, at the same point, of the reflected wave allows the calculation of the position of the defect if the speed of sound in the medium is known. Since the use of a continuous wave input would not allow differentiation between one flaw and another, it is more beneficial to use wave pulses of finite duration.

The equipment utilized in this test method consists of a transmitting probe, a receiving probe, and an electronic means of measuring time (usually an oscilloscope). Of course, proper electrical circuitry is necessary to provide the source pulse and to amplify the received signal. The receiver and transmitter probes can be combined into a single probe for convenience.

The Shadow (Transmission) Method. This test method is the oldest application of ultrasonic waves for non-destructive testing, dating back to 1930. The basics of this method are shown in Figure 10.

This testing procedure utilizes through transmission of the pulse in the material. A receiving crystal is placed on the side of the test material opposite that of the source crystal. Any discontinuity in the path of the wave causes a decrease in intensity of the wave at the receiver. A comparison is then made with the intensity received through a flawless specimen. Again, pulsed waves are used to avoid formation of standing waves in the test material. One of the most important advantages of the shadow technique is that there is no lower thickness limit for the test sample. This makes the method an excellent technique for the examination of thin laminated sheets. Another advantage is that it simplifies the examination of materials which have large grain size and uneven surfaces.

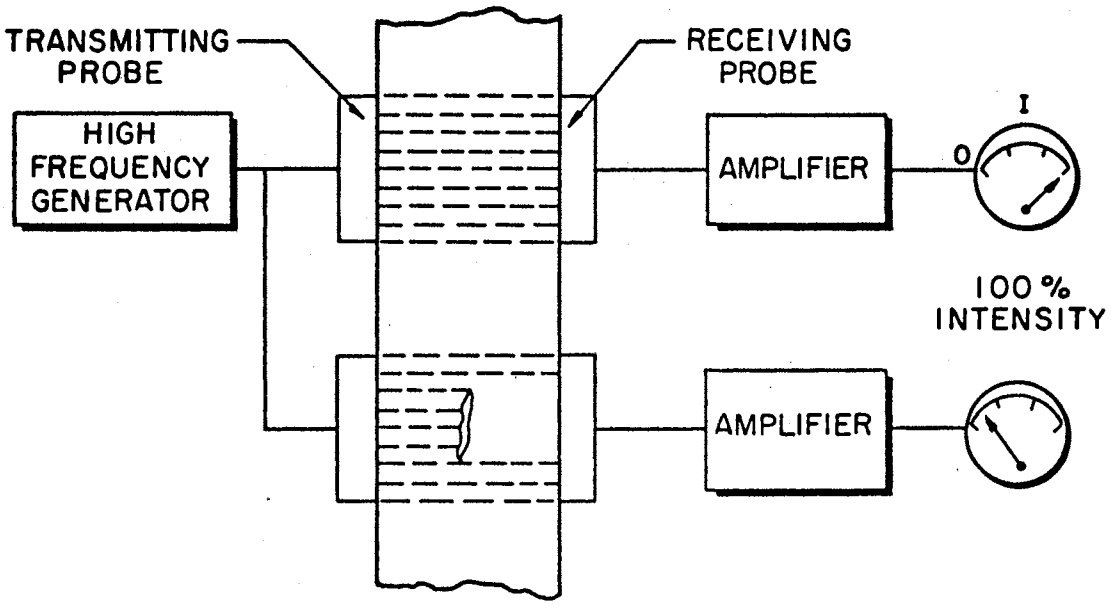

Figure 10. Shadow (Transmission) Method

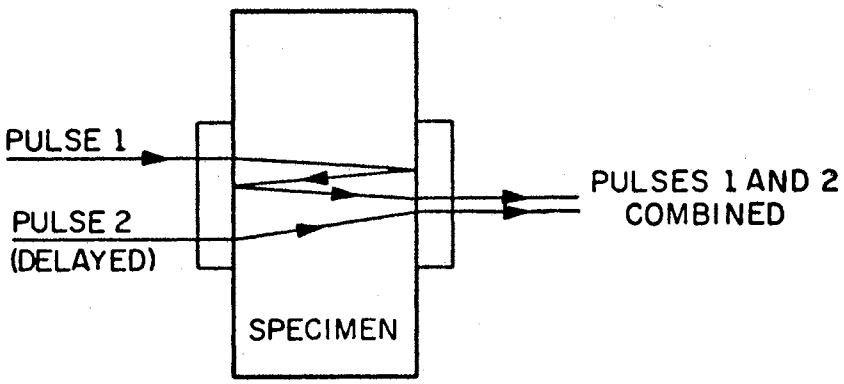

Figure 11. Interference Method

There are two principle limitations to this test. First, opposite sides of the test material must be accessible and the probes must be directly opposed to each other. The other drawback is that the exact position of the flaw cannot be determined.

The Resonance Method. This technique depends upon the reflections of ultrasonic waves from discontinuities. Resonance results from the fact that sound waves of definite length, on being reflected back and forth in the test material, are superimposed exactly in phase, whereas other waves cancel each other. Therefore, at resonance, maximum stress amplitude occurs. This resonance is influenced by the test material, the shape and dimensions of the test piece, the type and point of excitation and the mounting of the specimen. However, if all test conditions remain constant, a change in material properties can be determined by comparative measurement.

Since small flaws will not produce an appreciable effect on the resonance and since flaw position and size cannot be ascertained, this method is used primarily for thickness measurements. By measuring the frequency difference, Δf, between two successive resonance peaks, the plate thickness can be determined from the following relationship:

$$d = \frac{c}{2\Delta f}$$

where:

d = plate thickness

c = known velocity of sound in the plate

Δf = successive resonant frequency difference.

Material Property Evaluation

Ultrasonic testing also allows the investigation of those properties of the material structure that affect the propagation velocity and attenuation of ultrasonic waves. Velocity measurements and attenuation measurements will be considered separately.

Velocity Measurements. The relationships between the various elastic properties of materials and ultrasonic wave velocities have been derived in Appendix A and were presented earlier in this chapter. The elastic properties determined from wave velocity measurements, i.e., ultrasonic elastometry, are called dynamic constants.

The methods of testing for ultrasonic wave velocities are intimately related to ultrasonic flaw detection techniques discussed previously. They are usually divided into two categories, i.e., pulse echo methods and continuous wave methods.

Several variations of the pulse echo technique have been used for wave velocity measurements. The first of these methods is the direct transmission of ultrasonic wave pulses using time delay. This method utilizes a cathode ray oscilloscope to measure the time lapse between the actuation of the source transducer and the detection of the generated wave at the receiver. Simultaneously with the transmission of the pulse, the time base on the oscilloscope is triggered. When the wave is received, it is displayed as a vertical deflection of the oscilloscope trace. A measurement of the time from the onset of the time base to the time of the vertical deflection caused by the wave arrival at the receiver gives the travel time for the wave. Velocity is then calculated by the equation:

$$v = \frac{\ell}{t}$$

where:

v = velocity of wave

ℓ = path length

t = time of travel.

One of the major advantages of this method is that by transmitting directly from the source to the receiving crystal, the attenuation of the wave is kept to a minimum. Ergo, this approach is excellent for a highly attenuating test material.

Interference methods have been shown to be preferable to pulse delay methods in testing thin specimens. Several testing methods using this procedure exist. The basic technique is shown in Figure 11. An ultrasonic pulse is introduced from the transmitter and the pulse reflects back and forth in the test material between the source and receiver transducers. After a proper delay time, a second pulse is introduced into the specimen. The delay time is adjusted so that the first pulse is detected at the receiving crystal one echo transit time ahead of the second pulse pattern. These two pulses can be made to interfere in such a manner that they cancel each other. The velocity can be calculated using the following equation:

$$v = 2\ell\Delta f$$

where:

v = wave velocity

ℓ = sample length

Δf = frequency change between two successive in-phase transmissions (resonances).

The so-called "sing around" technique actually measures pulse repetition rate rather than wave velocity. The first returned echo is used to refire the transmitter for the second echo train. The repetition rate of the transmitter is, therefore, a direct function of echo transit time.

Of the continuous wave methods, by far the most important are those utilizing resonant frequency determinations. Wave velocities may be evaluated from specimens of known thickness using the phenomenon of resonance. The source transducer is applied to the specimen and the resonant frequencies of the standing wave are determined using a receiving crystal that indicates loading or deflection. For two neighboring resonant frequencies:

$$v = 2\ell\Delta f$$

where:

v = wave velocity

ℓ = thickness of specimen

Δf = frequency interval between two adjacent resonances.

Another continuous wave technique worthy of note is the frequency modulation method. This method uses continuous waves whose frequency is varied periodically. A wave that is reflected from the backwall of the specimen arrives at the probe after a travel time t, with a frequency f_0 at the moment of arrival, followed by a frequency rising to f_1. By monitoring the elapsed time between the generation of a wave whose frequency is the same as the received wave and the reception of the reflected wave, the travel time t is ascertained.

Attenuation Measurements. Attenuation measurements are, more often

than not, made from instruments that also allow velocity determination. Therefore, the testing techniques themselves are not unique, but the quantity measured is different from that of velocity determinations. One usually measures relative attenuation rather than attempt quantification of attenuation per se. The reason for this is that attenuation is usually measured as a function of wave amplitude. This amplitude, however, is not only affected by the attenuating properties of the test material, but by a number of other factors as well.

In the pulse echo technique, attenuation is calculated by comparing the amplitudes of successively reflected multiple echoes in the test material. The coefficient of attenuation is obtained from the formula:

$$\alpha = \frac{1}{2\ell} \ln \frac{1}{S_1 + S_n}$$

where:

α = attenuation coefficient

ℓ = thickness of specimen

S_1 = the ratio of the amplitude of the second pulse to that of the first pulse

S_n = the ratio of the amplitude of the $n + 1$ pulse to that of the n^{th} pulse where $n = 2, 3, \ldots$

In the transmission method, attenuation is measured by comparing the amplitudes of pulse traveling through different thicknesses of the test material or through the test material and a standard material. The tests are usually done with the specimen immersed in a liquid bath. The attenuation coefficient α is then calculated from the equation:

$$\alpha = \alpha_0 + \frac{1}{\ell_2 - \ell_1} \ln \frac{A_1}{A_2}$$

where:

α = attenuation coefficient of test material

α_0 = attenuation coefficient for liquid in which the specimen is immersed.

A_1 = pulse amplitude after passing through specimen thickness ℓ_1

A_2 = pulse amplitude after passing through specimen thickness ℓ_2.

Continuous wave methods are seldom used for attenuation measurements, primarily because the reflected waves can interfere with the incident waves. The interference can be eliminated by using transducers with attenuating covers. If one defines the maximum and minimum transmission coefficients $\alpha_{t_{max}}$ and $\alpha_{t_{min}}$ as the ratios of maximum reflected amplitude to initial amplitude and minimum reflected amplitude to initial amplitude, respectively, then:

$$\alpha = \frac{1}{\ell} \ell n \frac{\alpha_{t_{min}}^{-1} + \alpha_{t_{max}}^{-1}}{1 + (1 + \alpha_{t_{min}}^{-2} - \alpha_{t_{max}}^{-2})^{1/2}}$$

where:

α = attenuation coefficient of test material

ℓ = specimen length.

CHAPTER IV

TESTING DETAILS

Equipment

Electronic Equipment

The electronic equipment utilized to generate and to detect ultrasonic waves consisted of a pulse generator, source and receiver piezoelectric ceramic transducers and an oscilloscope. This equipment is shown in Figure 12.

The pulse generator delivered a high voltage (1100 volt), direct current spike pulse at a frequency of 60 hertz to the source transducer by the discharge of a condenser through an RCA 6130 hydrogen thyratron tube. A picture of the source pulse is shown as Figure 13. The pulse duration is .35 milliseconds. For optimum operation, other investigators have found that a source pulse duration in the order of 1 microsecond should be used. This is particularly important for identification of secondary echoes of the pulse. However, in this study, the primary interest was in the arrival of the first direct path wave pulse and this drawback was considered to be of minor concern.

The pulse generator also provided a trigger pulse of 11 volts DC to the horizontal time base of the oscilloscope. The trigger pulse occurred concurrently with the main voltage spike. The generator was developed by Professor A. M. Gaddis, formerly of Texas A & M University

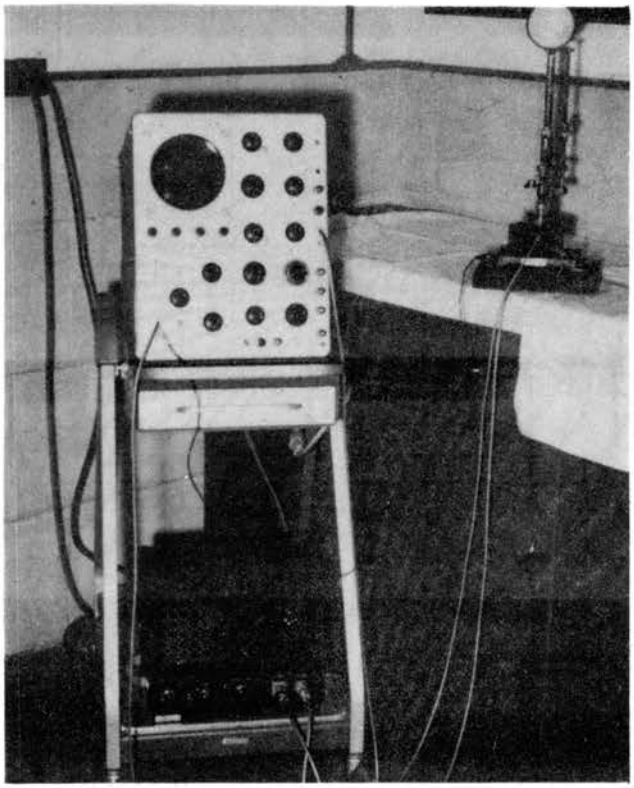

Figure 12. Testing Apparatus

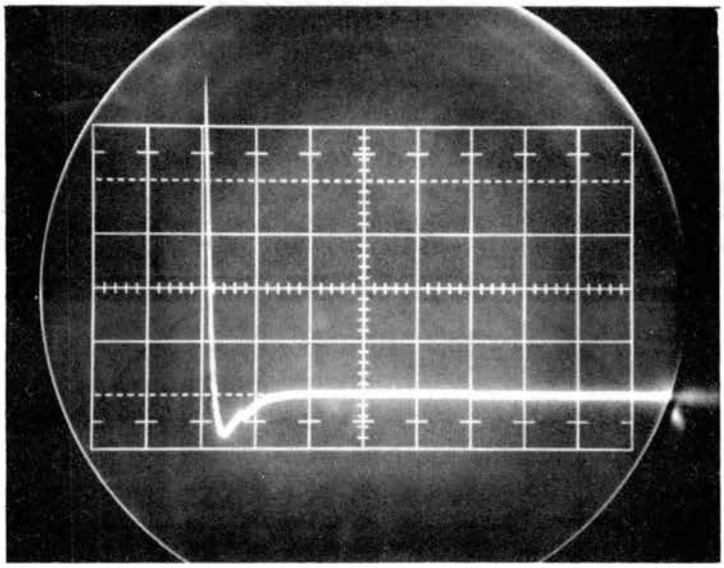

Figure 13. Trace of Source Pulse

and is not commercially available. A schematic wiring diagram of the pulse generator is shown in Figure 14.

The compressional and the shear wave transducers were piezoelectric ceramics manufactured by Gulton Industries. This ceramic material is a composition of lead zirconate titanate (PZT) and is identified by Gulton as HST-41. A summary of the specifications for this material is given in Table II.

The compressional ceramic discs had a diameter of 1.0 inch, a thickness of 0.25 inch (Figure 15) and were poled to be thickness expanders. The resonant frequency for these discs was 308 kilocycles per second. The source compressional transducer was provided with a 2-inch backing of polyethelene rubber to serve as a damping material. The receiver was backed by a lucite cylinder whose primary function was to provide a means of attaching the crystal to the holding device (Figure 16). A thin coating of silicone grease was used as a couplant between the transducers and the test specimen. This couplant provided excellent transmission of the compressional wave.

The shear mode crystals were constructed as 1.0 inch square plates with a 0.25 inch thickness (Figure 17). The shear plate thickness deformed into a rhombus upon excitation such that a shearing action was input into the test material. The resonant frequency of the shear plates was 172 kilocycles per second. Many different methods and materials were examined to determine the most suitable backing for the shear plates. Lucite and various thicknesses of rubber were among those tested. It was finally decided that a one-eighth inch rubber backing provided the best test results.

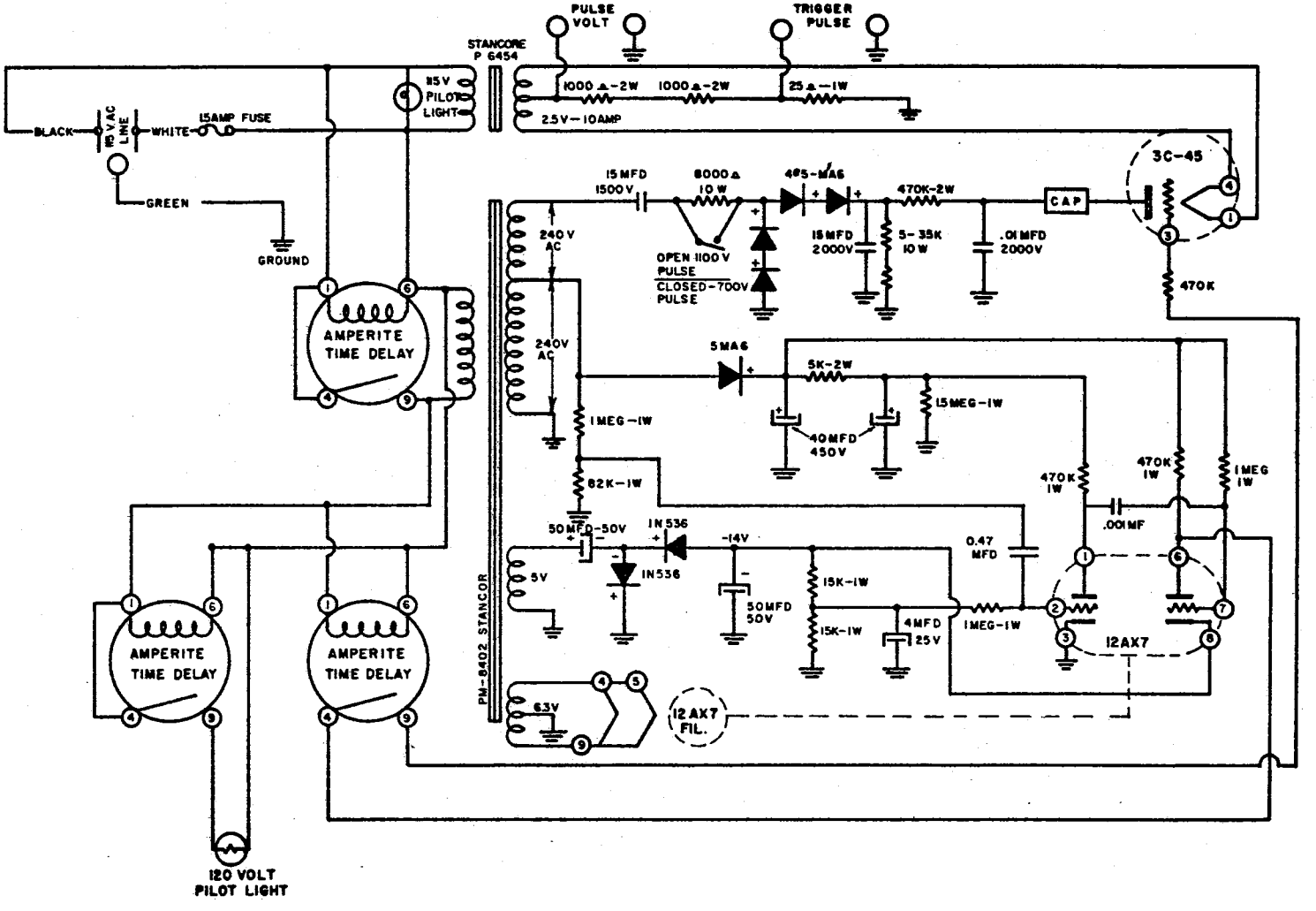

Figure 14. Schematic Wiring Diagram of Pulse Generator

TABLE II

SPECIFICATIONS OF GULTON HST-41 CERAMIC

Free Dielectric Constants		
k_3	1800	
k_1	2100	
Loss Tangent	.022	
Density	> 7.6	(gm/cm^3)
Curie Temperature	> 270	(^oC)
Coupling Coefficients		
k_{33}	.66	
k_p	.59	
k_{31}	.35	
k_{15}	.69	
Piezoelectric Charge Coefficient		
d_{33}	325	(meters/volt X 10^{-12})
d_{31}	-157	" "
d_{15}	625	" "
Piezoelectric Voltage Coefficient		
g_{33}	22	(volt-meter/Newton X 10^{-3})
g_{31}	- 11	" "
g_{15}	37	" "
Elastic Moduli		
Y^E_{33}	5.9	(Newton/$meter^2$ X 10^{10})
Y^E_{11}	7.0	" "
Y^E_{55}	1.8	" "
Q_m	70	
E_c	14	(KV/cm 60 cycles)
P_r	23	(μ coul/cm^2)

Figure 15. Compressional Wave Crystals

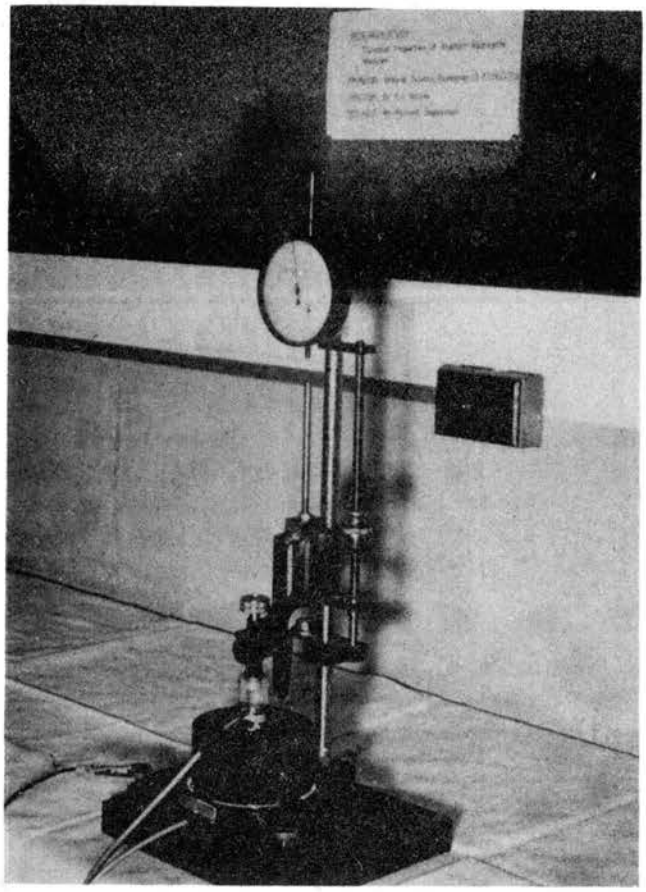

Figure 16. Holding Device With Specimen in Place

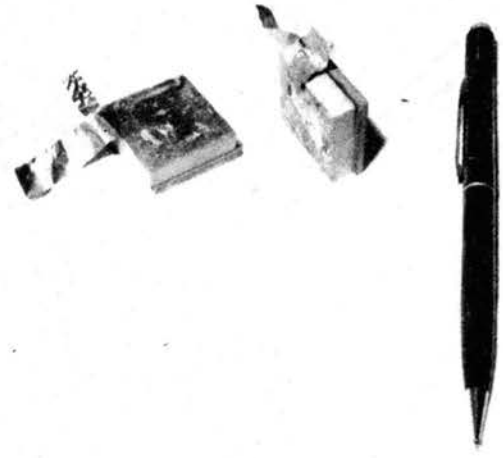

Figure 17. Shear Wave Crystals

It was determined that pressure coupling of the shear transducer to the test specimen enabled good transmission of the wave into the material under test. No intermediate coupling media was utilized.

Both sets of crystals were electroded on their two largest surfaces by a thin plating of a silver alloy affixed by the manufacturer. Leads of thin brass shemstock were attached to the electroded surfaces by soldering.

The cathode ray oscilloscope was a Tectronix Type 545B with a Type B wide-band, high gain preamplifier plug-in unit. The instrument had two time-base generators (A and B) with delayed sweep operation ability. Time measurements were made using the delayed sweep operation. By operating the horizontal display in the 'B intensified by A' mode, a portion of Time Base B was intensified during the time that Time Base A (the delayed sweep) was in operation. Using the B Time/cm or Delay Time switch in conjunction with the Delay-Time Multiplier, the beginning of the A sweep could be delayed so that it would occur at any point desired on the B sweep. In this manner, the time from the beginning of the B sweep to any point on the trace could be determined by adjusting the A sweep to begin at that point and recording the delay time as read from the dial settings (Figure 18). This method of measurement has the advantage of being independent of the horizontal sweep linearity. This technique allowed time measurements to be made to an error of ± 2 division of the Delay-Time Multiplier dial on the oscilloscope. The preamplifier had a vertical deflection sensitivity of 0.005 to 20 volts per centimeter and a horizontal time base sweep rate of 2 microseconds per centimeter to 1 second per centimeter with an accuracy of ±3%. The rise time of the preamplifier unit was 18 nanoseconds (10^{-12}).

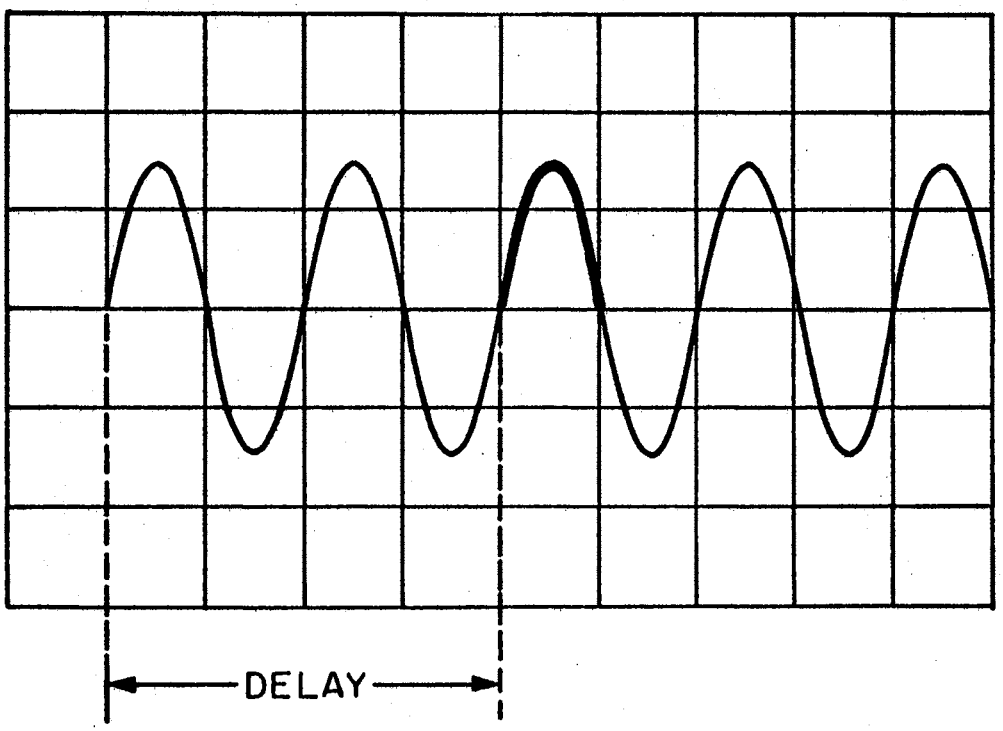

B TIME/CM or DELAY TIME Switch Setting X DELAY-TIME MULTIPLIER Dial Setting = Amount of delay between the start of the B (delaying) and the start of the A (delayed) sweep.

Figure 18. Time Measurement on Oscilloscope Using Delayed Sweep (From Textronix, Inc. Manual)

Temperature Monitoring Equipment

Variations in the temperature of asphalt concrete have been shown to influence ultrasonic wave velocities significantly. Consequently, it was deemed necessary to devise a method by which accurate determinations of test specimen temperature could be made concurrently with pulse velocity readings.

It was decided that a thermistor implanted in the test specimen itself would yield the best results. A thermistor is a semiconductor which exhibits large change in resistance with temperature. Their small size (Figure 19) and adaptability to remote readout devices made them ideally suited to the needs of this study. The thermistors chosen for this work were YSI Model 44004 manufactured by Yellow Springs Instrument Company. They have a working range of -112°F to 270°F.

The remote readout instrument was essentially a galvonometer which measured current change across the variable resistance thermistor. Calibration of the dial to indicate temperature enables direct readings of the temperature at the thermistor location. The output devices selected were also manufactured by YSI and, of course, were compatible with the thermistors. They are known as YSI Thermistemp TeleThermometers. The TeleThermometers chosen were Model 47TE. One TeleThermometer had a working range of -10°F to 105°F and the other had a working range of 60°F to 212°F.

Lead wires connecting the thermistors to the TeleThermometers were within size 18 to 22 gage. A simple phone plug was used as a connector to the readout device.

The thermistors were implanted in the test specimens by drilling a one-eighth inch diameter hole to the desired depth, placing the

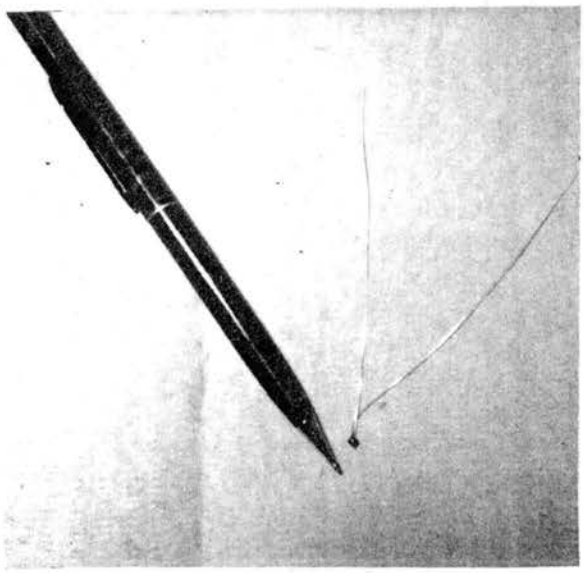

Figure 19. Thermistor

thermistor in the hole and then filling the hole with asphalt cement. The ends of the lead wires were left exposed for connection.

Preliminary work revealed that the temperature gradients between the center and the outer edges of the test specimens were insignificant. This was determined by implanting thermistors at varying depths and locations within the specimen and observing the temperatures as the specimen temperature was varied over the entire testing range. Consequently, it was decided that one thermistor located at mid-depth and just off center of the specimen would yield sufficiently accurate temperatures. It was also determined that a thermistor placed in this location would not interfere significantly with the transmission of the sound pulse. Figure 20 shows the TeleThermometer, lead wire and sample specimen with thermistor in place.

Environmental Control Equipment

The sample specimens were heated to a maximum test temperature of 170°F. This was accomplished using a Blue M Model OV-520C-1 forced draft oven with an operating range of 100 to 500°F.

A Lab-Line Model 3922 Controlled Temperature Cabinent with a maximum cooling capacity to -150°F was used for cooling of the test material. Minimum temperature used in these tests was -10°F.

Sample Preparation Equipment

The equipment used for preparation of the asphalt concrete specimens consisted of a mixer, a motorized gyratory-shear molding press and standard Marshall compaction equipment.

A Model C-100 Hobart Mixer was used to mix the asphalt with the

Figure 20. Temperature Monitoring Apparatus With Sample Specimen

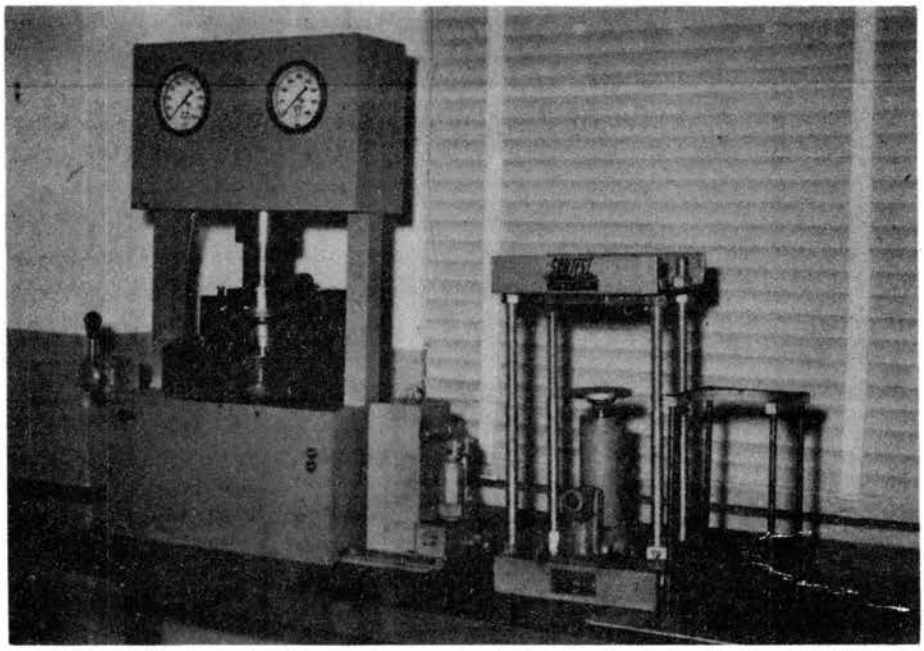

Figure 21. Motorized Gyratory-Shear Compactor

aggregate. The mixer was equipped with a whip beater for efficient mixing and to minimize aggregate degradation during the mixing operation.

The gyratory-shear molding press is shown in Figure 21. Compactive effort is applied by hydraulic pressure and rotation of the compaction mold which is held in a canted position. This imparts a kneading action to the material being compacted. The compaction process was continued until the densified asphalt-aggregate mixture had a certain resistance to load.

A dial gage mounted on a steel shaft was utilized to determine compacted specimen thicknesses or heights. Readings were made to the nearest .001 inch.

Materials

Aggregate

Three different aggregates were utilized in the asphalt concrete. All three (a fine sand, a coarse sand, and a crushed limestone) were obtained from a local hot mix asphalt plant.

Asphalt Cement

The asphalt cement used in this mixture was a 60-70 penetration grade steam and vacuum refined material. The specific gravity (at 77°F) of the material was 1.005 and it had a softening point of 118°F.

Sample Preparation

The aggregates were sized on U.S. Standard sieves and then recombined according to the Oklahoma Highway Department specifications for a

Type C surface course mixture (54). Figure 22 shows the combined grading of the aggregate mixture and the Type C specifications.

The aggregates and the asphalt cement were then heated to a temperature of 325°F. The heated aggregates were placed in the mixing bowl, the proper amount of asphalt cement added and the mixing accomplished using the Hobart Mixer.

The Hveem-gyratory specimens were compacted into cylinders four inches in diameter and two inches high. These specimens were molded using the gyratory-shear compactor. This method of compacting bituminous specimens has been standardized by the Texas Highway Department (Test Method Tex-206-F, Part II). Different densities, i.e., void contents in the compacted specimens were achieved by varying the compactive effort expended in the molding process.

Hveem specimens were made with asphalt contents varying from 4% to 8% by total weight of the mixture. Specimens at 5% asphalt content were compacted at void contents ranging from 1% to 11% by volume.

Other specimens were molded using the Marshall Compaction Method. This method produces a four inch diameter by two and one-half inch high specimen. In this procedure, each face of the specimen was subjected to 50 blows of a standard 10 pound hammer falling 18 inches. Specimens were compacted by this process at asphalt contents ranging from 4 to 6% by total weight.

Testing Procedure

General

The advantages of examining asphalt concrete ultrasonically have been discussed earlier in this paper. Several investigators, as

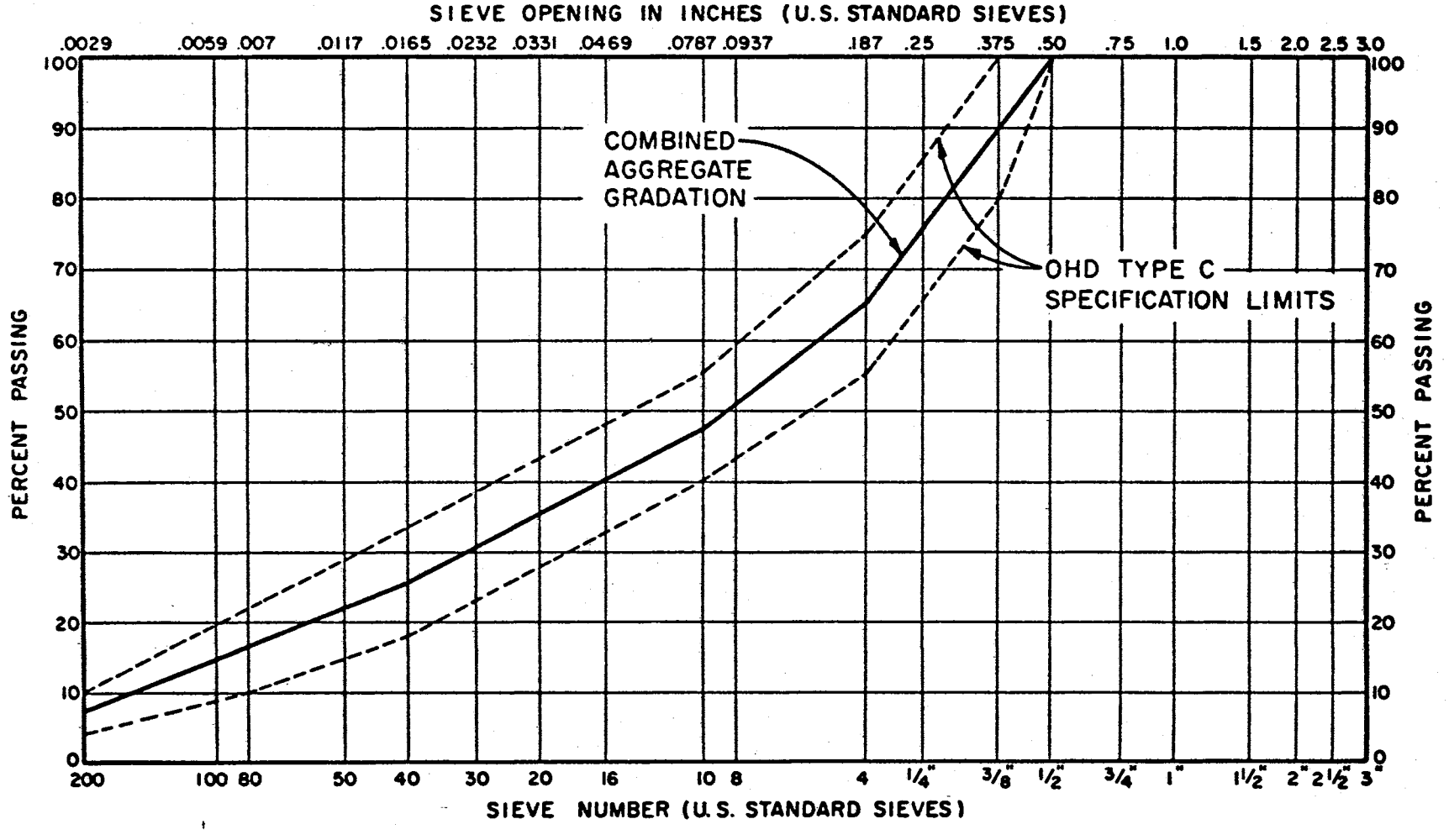

Figure 22. Combined Aggregate Grading Chart

previously noted, have pioneered work in this area. Goetz (9) used a resonant frequency technique to measure longitudinal wave velocities in asphalt concrete beam specimens. Manke and Galloway (32) employed a pulse technique to also measure longitudinal wave velocities in standard size asphalt aggregate samples. Previous work done by the author (46) utilized pulsed longitudinal waves to investigate the temperature-dependent properties of asphalt concrete. However, up to this time, no pulse technique for measuring transverse wave velocities in asphalt concrete has been devised or at least no reference to such a technique was found in a rather extensive literature review. The need for such procedures has been pointed out in various studies. Measurement of the velocity of the transverse wave through asphalt concrete, in conjunction with similar measurements of the longitudinal wave velocity, would allow the calculation of several important elastic constants that are descriptive of the dynamic nature of the test material. The technique presented in this study should provide the highway engineer a new means by which the dynamic behavioral tendencies of asphalt-aggregate mixtures can be analyzed nondestructively.

The inherent inhomogeneity of asphalt concrete and the high attenuation of ultrasonic waves passing through this material, as well as the self-imposed restriction of testing specimens compacted by standard methods to standard sizes, necessitated techniques differing from the standard procedures used with other, more homogeneous materials. The large grain sizes of some of the aggregate in the specimen required longer wave lengths than are usually employed. The scattering caused by the large aggregate grains and the viscous nature of the asphalt binder required a wave of relatively large amplitude to overcome the

attenuation tendencies of the material. The longer wave length, in turn, does not allow sharply collimated sound beams as is customary in metal testing. In addition, all three types of wave modes (compression, shear, and surface) are excited no matter what the polarity of the source transducer might be. This occurs because of the elastic nature of the piezoelectric crystal and the surface irregularities at the transducer/specimen interface. Due to the high attenuation and scatter in the material, identical source and receiver transducers were used. The receiving transducer was placed directly opposite to the source transducer (direct transmission method).

The ultrasonic compressional wave travels with a greater velocity of any of the other wave modes. If an ultrasonic wave is input at one face of the test specimen, the first motion detected by the receiver on the diametrically opposite face will be the arrival of the compressional wave. Other wave modes, as well as reflected and refracted compressional waves, will arrive later in time than the original wave traveling a direct path between the two transducers. This is due to their longer path lengths and/or slower characteristic velocities. Figure 23 is a schematic diagram of the test set-up showing the first pulses of different waves. The reception of the direct path longitudinal wave (L_1) is followed by the reception of the transverse (T_1) and surface waves (S_1). These waves may be distorted by the reflected and refracted longitudinal waves (L_2, L_3, etc.). The numerous large aggregate grains further complicate the output pattern due to multiple wave reflections and refractions at their boundaries.

Because of the manner in which the specimen is supported in the holding apparatus, only a small portion of the wave energy is lost at

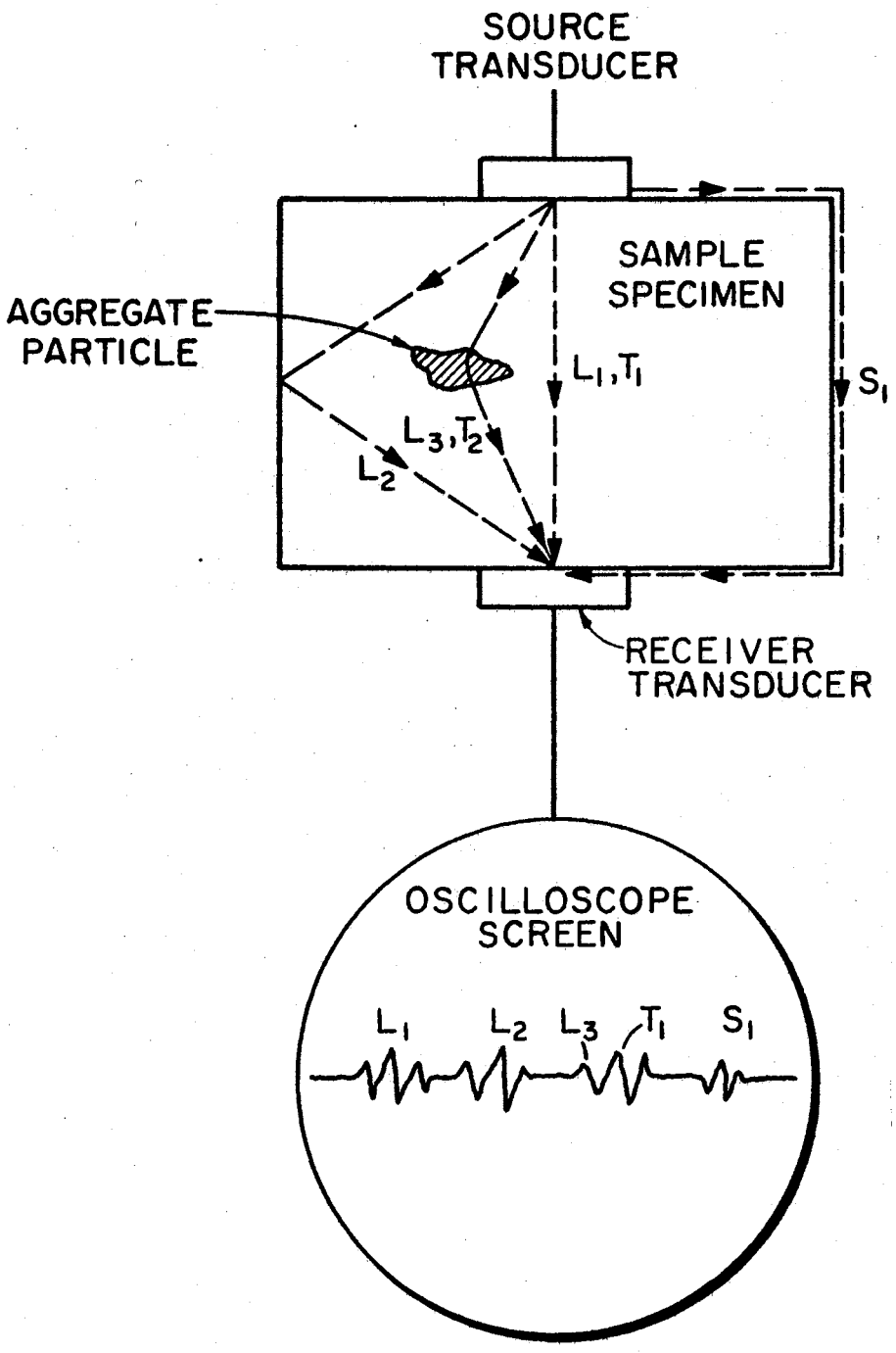

Figure 23. Schematic Diagram of Ultrasonic Wave Paths and the Trace Indication of Their Reception

the receiver face of the sample. The portion of the wave not transmitted to the receiver itself strikes the specimen/air interface and is reflected back toward the source face of the specimen (Figure 24). At the source surface, the wave is again reflected and travels back to the receiver transducer. This reflected wave arrives at the receiver at a time equal to 3 times t. Reflection continues in this manner until the wave source is shut down and the wave itself is damped to zero amplitude.

Two separate types of tests were made in this study. The first type employed the longitudinally poled transducers to generate a relatively high amplitude compressional wave and lesser amplitude waves of other modes. The second test type used the transversely poled transducers to input a wave of a primarily shearing mode.

Longitudinal Wave Velocity Measurements

Figure 25 is a photograph of the oscilloscope trace of a wave transmitted through a 4% asphalt concrete specimen using the compressional transducers. The major particle motion occurs in the longitudinal mode due to the crystal polarity, hence the compressional wave travels through the test material with a relatively large amplitude. Therefore, the receiver, also poled longitudinally, detects the longitudinal wave not only as the initial particle motion, but also as a large amplitude disturbance. By this reasoning, point A on Figure 25 is the point in time when the direct path compressional wave arrives at the receiver, (t_{L1}). As discussed above, the wave reflects between the two parallel surfaces. Consequently, points D and E in Figure 25 correspond to 3 times t_{L1} and 5 times t_{L1}, respectively.

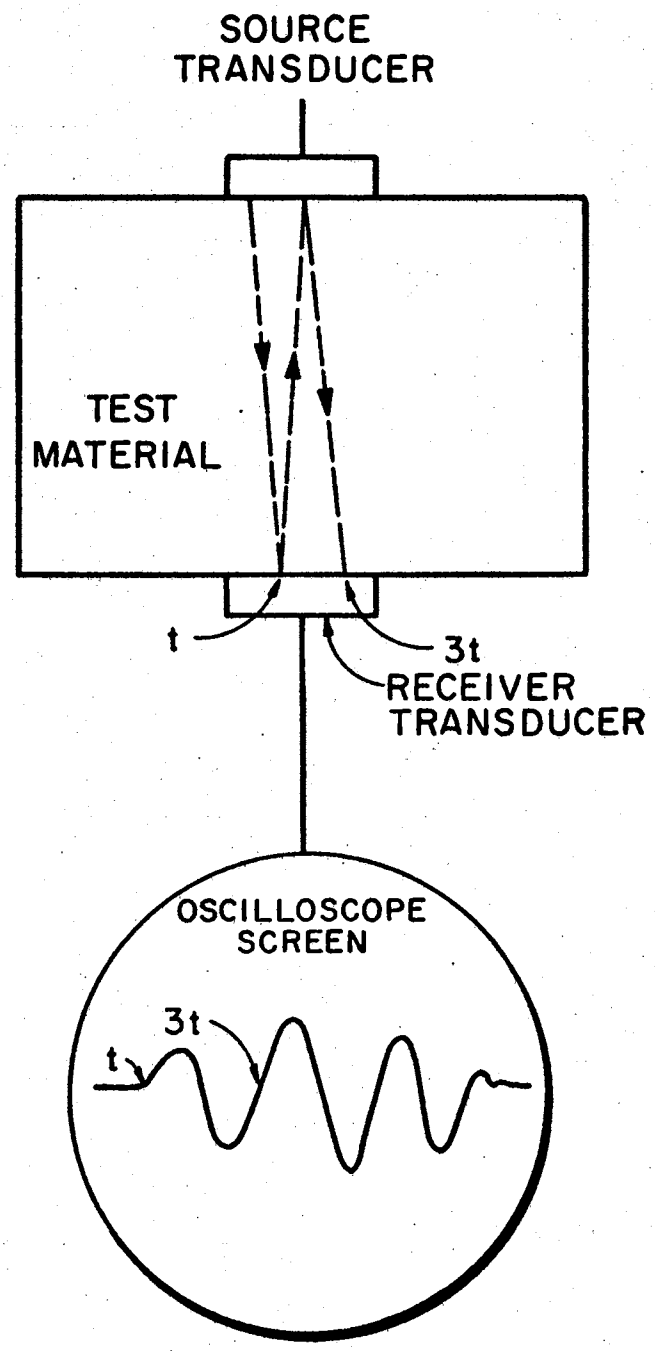

Figure 24. Schematic Diagram Showing Reflection of Waves in Test Medium and Schematic Scope Trace

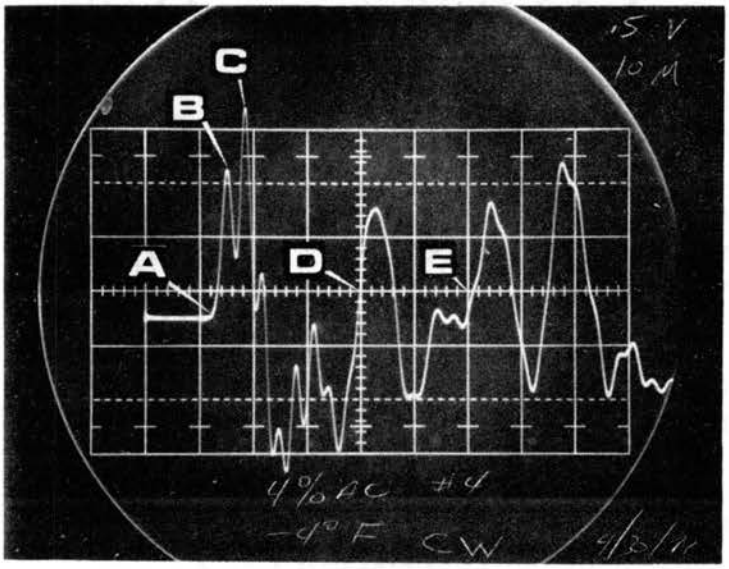

Figure 25. Oscilloscope Trace of Longitudinal Wave Through 4% Asphalt Concrete

Simultaneously with the longitudinal reflections in the material, the source crystal is resonating because of the length of the driving pulse. This behavior inputs a low amplitude wave with a frequency approximately equal to the resonant frequency of the crystal. Referring again to Figure 25, the period of the high frequency wave as measured from point B to point C is approximately 3.3×10^{-6} seconds. This corresponds to a frequency of 303 kilocycles per second. This frequency agrees well with the calculated resonant frequency for the transducers of 308 kilocycles per second. During this time, both reflected and refracted waves of different modes, as well as the direct path shear wave, are striking the receiver. However, the arrival of the direct path shear wave was sufficiently masked by the extraneous indications so that it was not definitely distinguishable on the trace.

Transverse Wave Velocity Measurements

Shear wave velocities were more difficult to determine than were the compressional wave velocities. The basic problem in the measurement of shear wave velocity stems from the high attenuation of the shear wave in asphalt concrete, the consequent necessity of inputting a high amplitude wave, and the difficulty of securing good transducer/test specimen coupling. Therefore, piezoelectric transducers operating in primarily a shear mode were needed to enable generation and detection of the shear wave.

Unlike the compressional wave testing procedure, the first particle motion to arrive at the receiver will not be the same mode as the major input. Although the major input mode is shear, Poisson's effect will also cause small amplitude compressional waves to be introduced into the

specimen. These waves, traveling with a greater characteristic velocity, will arrive at the receiver before the larger amplitude shear wave. Other compressional waves, originating through mode conversion as the shear wave impinges upon materials having different acoustic impedances, will also arrive ahead of the shear wave. If the original shear wave amplitude is not great enough, its arrival at the receiver will be masked by the other extraneous indications.

In this type of test, the transversely poled transducers were used to generate a relatively high amplitude shear wave in comparison with the other accompanying wave forms. Figure 26 is a photograph of an oscilloscope trace output from an asphalt concrete specimen tested with these shear transducers. The low amplitude, high frequency precursor displayed in the initial portion of the trace is not fully understood at this time. It was found not to be grass indication from the previous pulse and it did occur immediately with the firing of the source crystal. The precursor remained constant throughout the various tests and was not noticeably affected by temperature or the physical make up of the specimen. Again, because the major input wave particle motion occurs transversely, and since the receiver is poled to be most sensitive to the shearing mode, the direct transmission transverse wave appears on the output trace with a relatively large amplitude. While the direct transmission longitudinal wave precedes in time the arrival of the transverse wave because of its higher characteristic velocity, the amplitude of the longitudinal wave is smaller compared to that of the transverse wave. Point A on the trace (Figure 26) is considered to be the point in time of the arrival of the longitudinal wave. Peaks B and C define a period of 6.0×10^{-6} seconds, corresponding to a

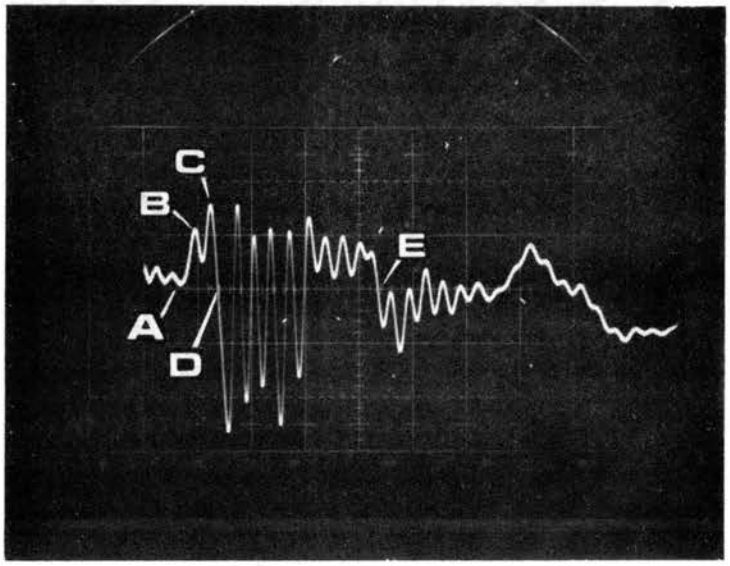

Figure 26. Oscilloscope Trace of Transverse Wave Through 6% Asphalt Concrete

frequency of 166 kilocycles per second. This frequency compares quite favorably with the resonant frequency of the transducers (172 kilocycles per second) indicating that these signals are caused by the resonating of the shear transducer. At first observation, point C appears to be a likely choice for the arrival of the transverse wave. However, it was found that increasing the test specimen temperature resulted in variations in this point. The point in time where the trace crossed the zero axis (point D) was selected to be the time of arrival of the transverse wave (t_{T_1}). This point was easily identifiable throughout the testing procedure. To determine if this point actually would indicate transverse wave arrival, tests on steel, lucite, and concrete were run and the results compared with results published by other investigators. Table III shows that the procedure outlined above did provide excellent agreement with known results.

Reflection of the transverse wave from the test material/air interface occurred in a manner similar to the reflection of the longitudinal wave. The amplitude of the reflected wave was much reduced due to the attenuation characteristics of the shear wave in the test media. Point E in Figure 26 is believed to be the arrival of the first reflected shear wave ($3 \times t_{T_1}$).

The operation of the test equipment in recording the travel time of the ultrasonic pulse was basically quite simple. The test specimen was placed on the holding device with its bottom face resting on the source transducer and the receiver transducer was positioned on the opposite face of the specimen. The pulse generator activated both the source transducer and the horizontal trace of the oscilloscope simultaneously. When a signal was perceived by the receiver, it generated a small

TABLE III

COMPARISON OF SHEAR WAVE VELOCITY MEASUREMENTS

	Transverse Wave Velocity (FPS)		
Source	Steel	Lucite	Concrete
Krautkramer	10,600	4,700	7,500*
Filipczynski et al.	10,600	3,700	7,000*
Stephenson	9,500	4,200	7,200

*The transverse velocity in concrete equals approximately one-half of the published values of longitudinal velocity.

voltage that was preamplified and fed to the vertical plates of the oscilloscope causing a vertical deflection of the trace. A measurement of the time lapse between the activation of the source transducer and the vertical deflection of the trace on the oscilloscope screen yielded the travel time. The velocity of the wave was simply the known specimen height divided by the observed travel time. Figure 27 is a schematic diagram of the test arrangement and the equipment components.

The measurement sequence for the full temperature range tests was to first cool the specimens to -15°F and then allow them to heat gradually until the terminal temperature of 160°F was reached. Test temperatures were monitored using the thermistors and travel time readings were made at 5°F increments over the entire range. Separate tests were made for longitudinal and transverse wave velocities.

Precision

The precision of the temperature readings was limited by the readout device. The available accuracy was approximately 1% of the scale span (1.5°F).

All of the travel time readings could be repeated to ± 2 divisions of the Delay-Time Multiplier dial on the oscilloscope. This was equivalent to a precision of ±1.5%.

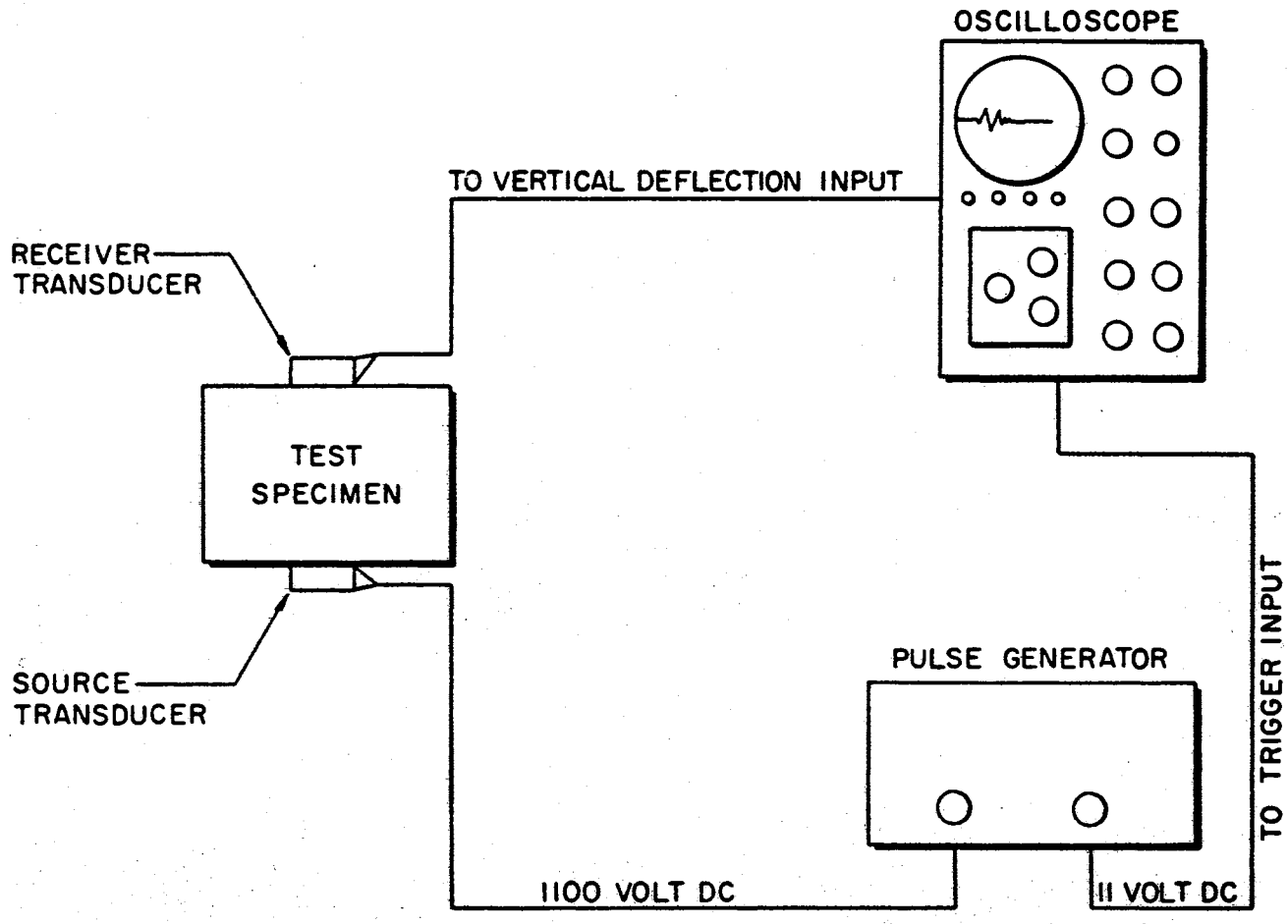

Figure 27. Schematic Diagram of Equipment Components and Test Arrangement

CHAPTER V

TEST RESULTS AND DISCUSSION

Introduction

The testing technique employed in this study would be advantageous only if it yielded results indicative of the actual dynamic properties of the material being tested. It was believed that if test results obtained in the manner previously described were compatible with the expected or predictable behavioral tendencies, and if they were consistent with the results obtained by other investigators using different testing procedures, that the usefulness of this technique would be confirmed. The effects of variations in temperature, asphalt content, and void content on the ultrasonic wave velocities in a specific asphalt-aggregate mixture were investigated. The changes in certain "elastic" constants of this material as calculated from the observed wave velocities were also determined. The following results are presented only as indicative behavior of the particular material tested.

Temperature Effects

Ten specimens, two each, with asphalt contents of 4, 5, 6, 7, and 8% by total weight, were continuously tested for compressional wave velocity as their temperature was increased from -15°F to 160°F. Internal specimen temperatures were monitored via the implanted thermistors and velocity readings were made at increments of 5°F.

Compressional Wave Tests

Figure 28 shows two photographs of the compressional wave traces for a 4% asphalt concrete specimen. The top trace was made with the specimen at a temperature of -4°F, while the bottom trace was made at 160°F. It is easily seen in these photographs that the arrival of the initial vertical deflection takes almost twice as long in the hotter specimen as in the colder specimen. Secondly, the amplitude of the received wave is greatly reduced when the specimen is at the higher temperature.

Figure 29 is a plot of average compressional wave velocity in feet per second (fps) versus temperature (°F). For clarity, the actual data points are not shown, but the uneven nature of the plots indicates a certain amount of scatter in the readings. This data scatter can be attributed to several factors. Nonhomogeneity of the aggregate particle sizes, shape, and orientation in the compacted specimens is, perhaps, the most obvious source of error. Random errors inherent in the measurement procedure, i.e., those related to the instrumentation and those pertaining to operator technique, could also be responsible for, or at least have some influence on, the scatter.

Despite the scatter, however, specimens at each of the asphalt contents exhibited the same general trend. As shown in the figure, the compressional wave velocity decreased with increasing temperature. The rate of decrease also increased as the specimen temperature was raised. The average velocity decrease exhibited by these mixtures was approximately 46% of their maximum (low temperature) velocity.

This decrease in compressional wave velocity with increasing temperature of the mixture was expected since previous investigators

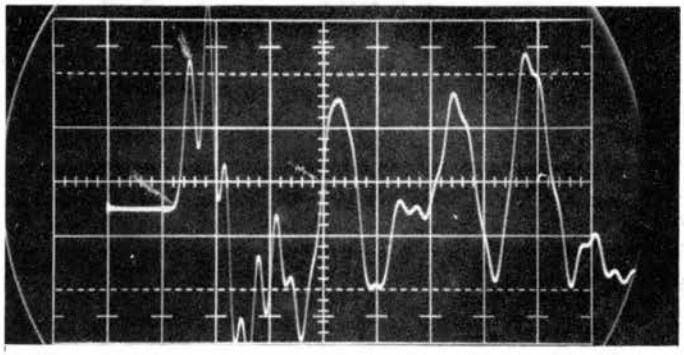

-4°F

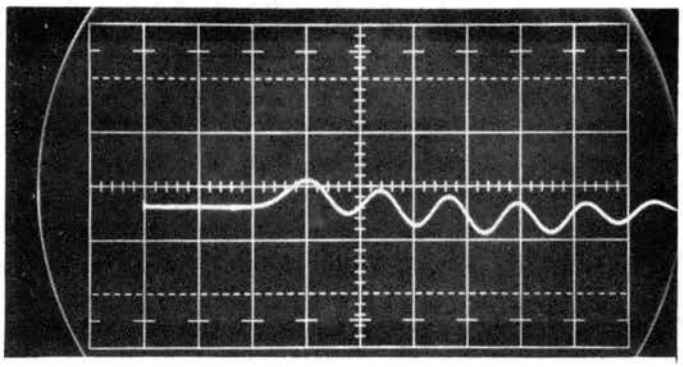

160°F

Figure 28. Effect of Temperature on Longitudinal Wave in 4% Asphalt Concrete
(Horizontal scale = 10 μsec/cm
Vertical scale = .5 v/cm)

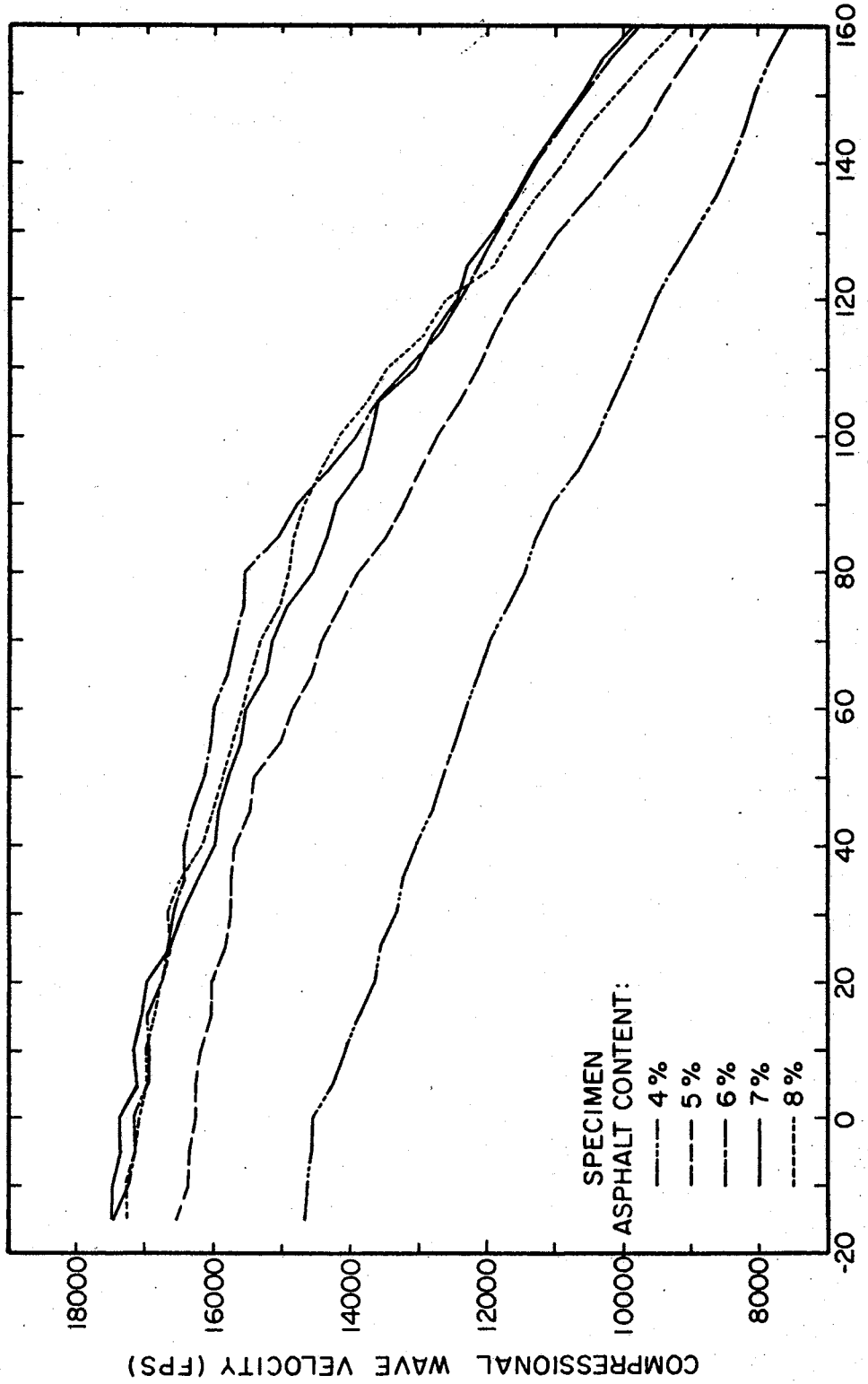

Figure 29. Compressional Wave Velocity Versus Temperature

(9) (32) have reported similar results. Previous work indicated that this tendency also holds for mixtures containing different grades of asphalt cement although the exact behavior pattern, with regard to rate of decrease in velocity, is probably characteristic of a given asphalt-aggregate mixture (46).

The behavior of an asphalt-aggregate mixture is complicated by the material deformation characteristics at various temperatures related to the consistency of the asphalt binder. At relatively high temperatures, the mixture may be a highly plastic (tending to viscous) material and, at lower temperatures, the mixture may be considered as an elastic material. Between these temperature extremes, the material will probably exhibit both elastic and plastic characteristics.

As temperature is increased, the viscosity of an asphalt cement will decrease, the material characteristics changing from a brittle solid to a semi-solid and finally, to a viscous liquid. In an asphalt-aggregate mixture, the films of asphalt surrounding the aggregate particles serve as a binder or cementing agent. As the nature of the films change with increasing temperature, the aggregate matrix is less tightly bound together, i.e., it becomes less rigid. Consequently, the mixture is unable to transmit the compressional wave at as high a velocity as it can at low temperatures.

It was expected that at some low temperature the compressional wave velocity would attain a limiting value. Although the curves do indicate a leveling off at lower temperatures, limitations of the temperature monitoring equipment prevented examinations below -15°F.

At the other temperature extreme, some minimum rate of travel of the compressional wave was also expected. However, beyond the

temperature of 160°F the specimens softened to such an extent that they fractured and spalled during the testing operation. Consequently, velocity measurements could not be made above this temperature.

Although instrumentation procedures were not developed to measure the attenuation of the compressional wave as it passed through the specimen, visual observations were noted. Compressional wave amplitude increased as the specimen temperature increased from -15°F to approximately 100°F. Above this temperature, wave amplitudes decreased until they became quite small. This phenomenon would indicate that there is a rather narrow range of temperatures at which optimum transmission of the wave energy occurs in a particular mixture. Less energy is lost through the mechanisms of scattering and absorption in this particular temperature range than at any other.

At low temperatures, the volume of the asphalt cement will decrease giving rise to minute increases in void spaces in the matrix. Although the cement is more rigid and does transmit the wave at a higher velocity, these discontinuities in the structure apparently reduce the amplitude of the transmitted wave. As the temperature increases, the volume of the asphalt increases and fills a portion of the discontinuities, thereby reducing the attenuation until an optimum temperature is reached. Beyond this temperature, the asphalt cement becomes so plastic that it severely attenuates the wave.

Variation of the temperature dependent characteristics of the ceramic transducer could also be an influencing factor on the wave attenuation. However, according to data supplied by the manufacturer, these are considered to be very minor within the range of test temperatures employed.

Shear Wave Tests

Figure 30 shows three photographs of shear wave traces for a 6% asphalt concrete specimen. The top trace was photographed at a specimen temperature of -15°F. The middle trace was photographed at a specimen temperature of 90°F, and the lower trace at a specimen temperature of 160°F. The arrival time of the large amplitude shear wave is readily seen to increase as temperature increases. Another unique feature is the increased wave amplitude at 90°F in relation to the other two traces.

Figure 31 is a plot of shear wave velocity (fps) versus temperature (°F). Again, some scattering of the data was encountered, although the trends of the plots for the various mixtures were consistent. This scattering is due to essentially the same causes as for that of the compressional wave-temperature results. Other error sources related to the instrumentation for shear wave velocity measurements have been discussed previously.

Figure 31 shows the same general behavior pattern as did the compressional wave velocity-temperature plot (Figure 29). That is, the shear wave velocity decreased with increasing temperature and the rate of decrease increased as the temperature was raised. Over the testing temperature range, the average velocity decrease as a percentage of the low temperature velocity was approximately 64%. This percentage decrease, although larger than for the compressional wave tests, is based on a smaller actual velocity change-approximately 5000 fps as compared to 7500 fps.

Over the test temperature range, the ratios of compressional wave velocity to shear wave velocity varied from 2.150 to 4.993. These

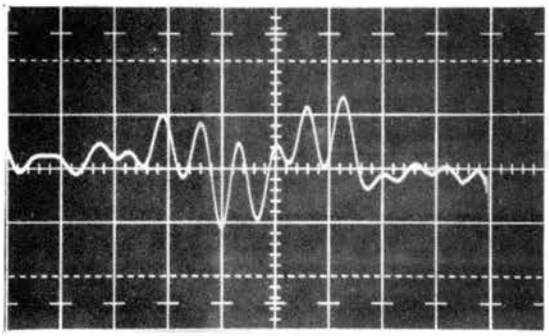

-15°F

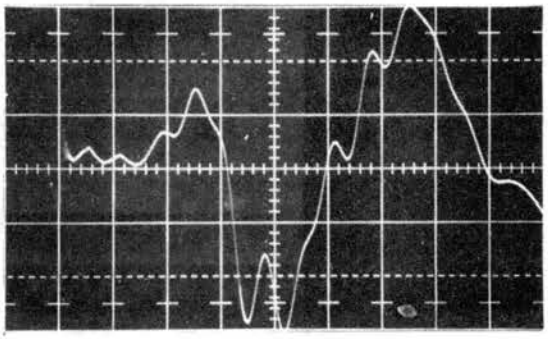

100°F

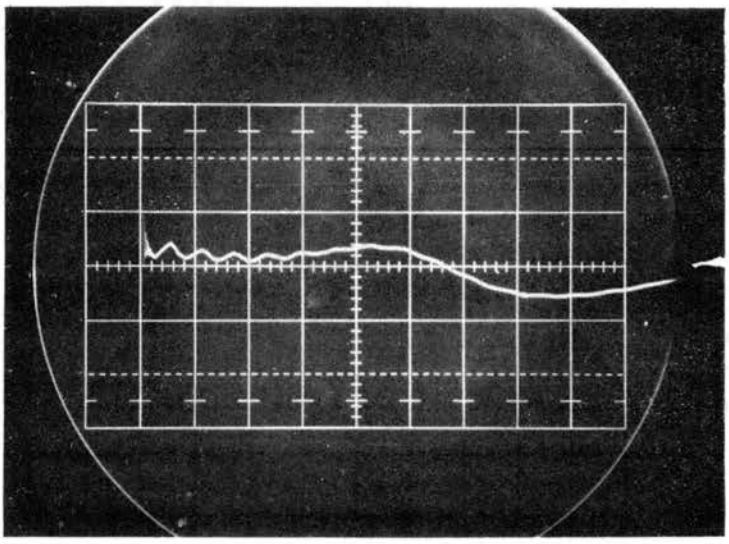

160°F

Figure 30. Effect of Temperature On the Transverse Wave in 6% Asphalt Concrete (Horizontal scale = 10 μsec/cm; Vertical scales = .1 v/cm)

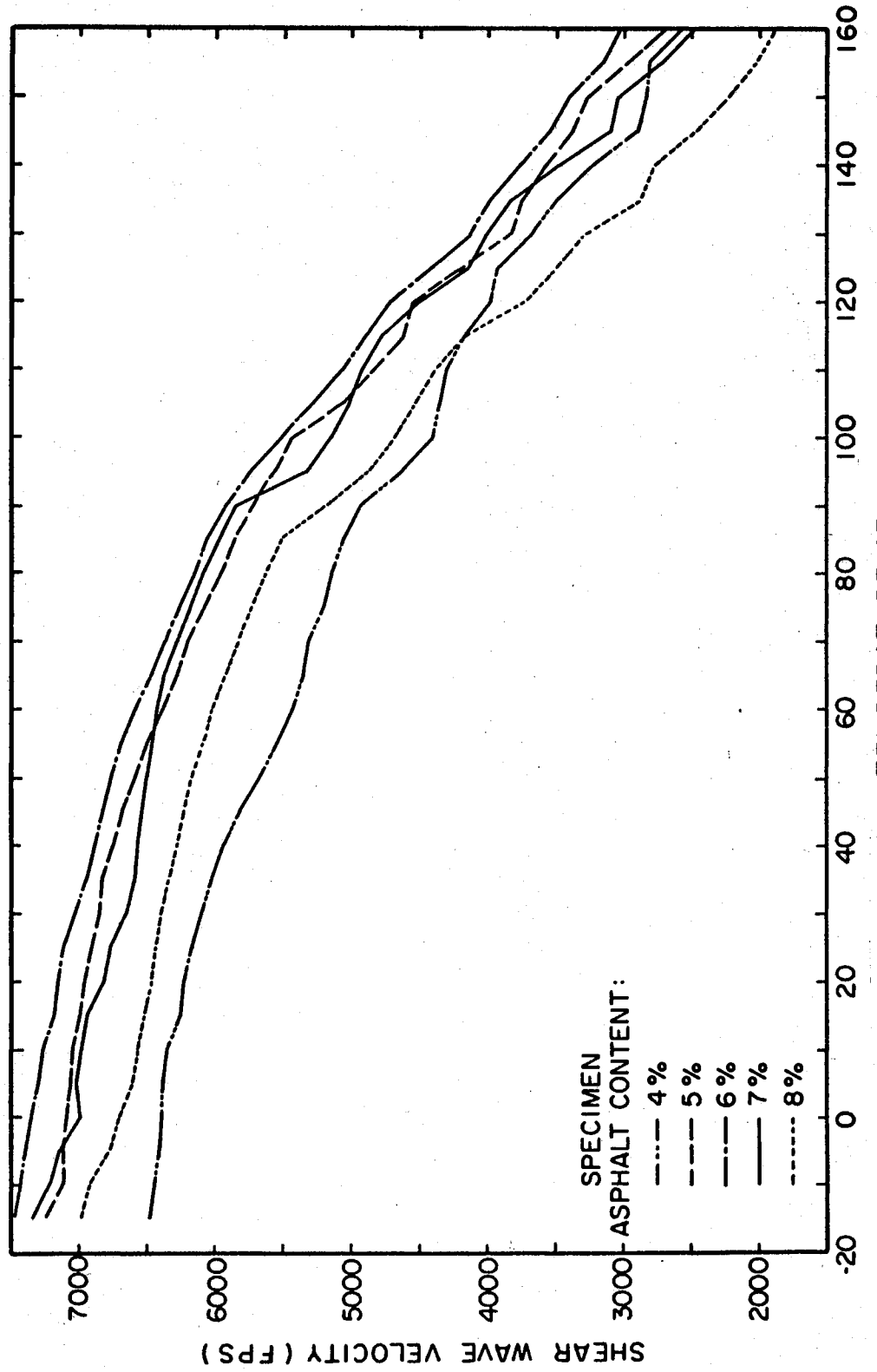

Figure 31. Shear Wave Velocity Versus Temperature

ratios indicate that the shear wave velocities determined by this method are reasonable since they are compatible with those predicted from elastic theory.

As illustrated in Figure 30, attenuation decreased until the specimen temperature was approximately 100°F. Beyond this temperature, the wave amplitude decreased drastically until the arrival of the wave became quite difficult to determine. Since the softening point of the asphalt cement used in this study was approximately 118°F, this could be another indication of the influence exerted by the viscous nature of the binder. The attenuation phenomenon is thought to occur in much the same manner as it does for the compressional wave.

Asphalt Content Effects

Although previous work indicated that wave velocity increased with increasing asphalt content considerably beyond that content normally considered as optimum for the mixture, the results of this study do not agree (46). In both the compressional wave velocity (Figure 26) and the shear wave velocity (Figure 27) tests, the velocity increased with asphalt content up to a limiting value in the area of 6%-7%. For the aggregate mixture used in this study, optimum asphalt content was 6.2%, as determined by the Hveem-Gyraton test data. Figure 29 is a plot of compressional wave velocity versus asphalt content for 0°F, 80°F, and 160°F. In both the low and the high temperature tests, the maximum compressional wave velocity occurred in the 7% asphalt content specimens. The velocity at 6% asphalt content is, however, only slightly less. At 80°F, the 6% asphalt content material has the greatest velocity. Figure 30 is a similar plot of shear wave velocity versus asphalt

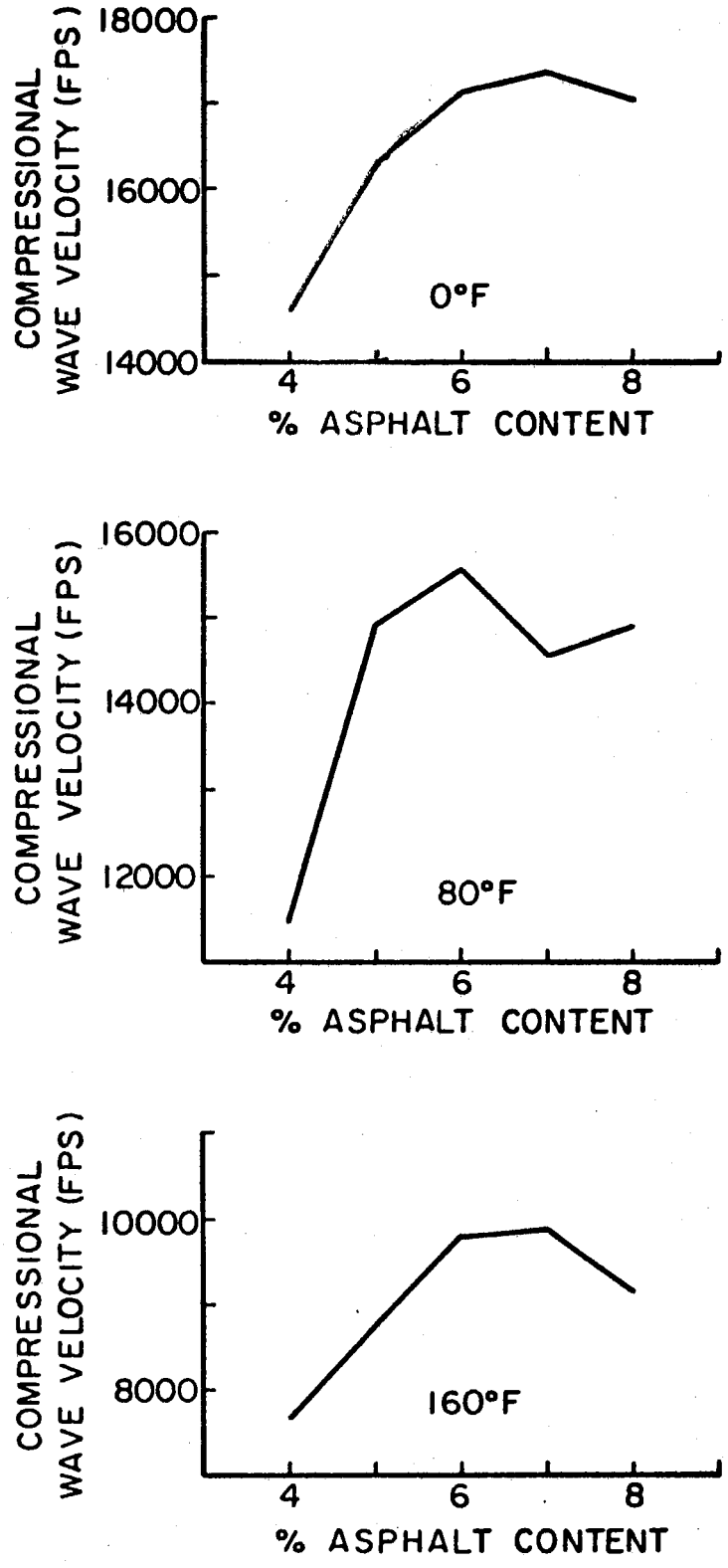

Figure 32. Effect of Per Cent Asphalt Content on Compressional Wave Velocity

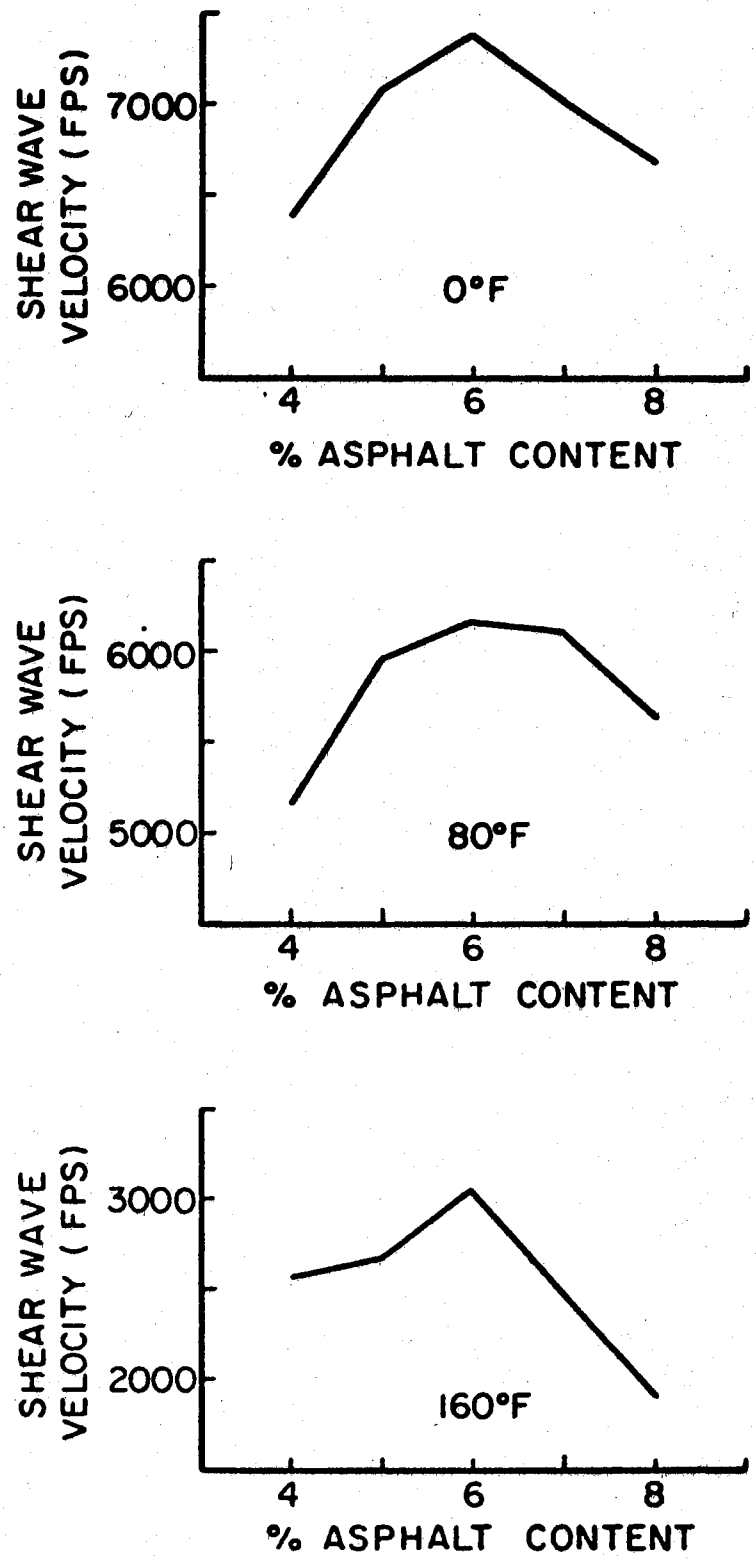

Figure 33. Effect of Per Cent Asphalt Content on Shear Wave Velocity

content for temperatures of 0°F, 80°F, and 160°F. In these curves, the maximum shear wave velocity occurred consistently in the specimens containing 6% asphalt cement.

No direct correlation of optimum asphalt content and maximum wave velocity could be made. However, these curves, while not conclusive for defining optimum asphalt content as defined by standard tests, do give an indication of the percentage of asphalt that yields the best conditions of inter-particle contact and minimum path length for the transmission of the wave. In a series of specimens compacted from design mixtures, conditions should exist where there is a sufficient quantity of asphalt cement to achieve optimum particle orientation and reduction of void content so that the pulsed wave can travel from aggregate particle to aggregate particle with only minimal travel distance through the acoustically slower asphalt binder. The use of lesser quantities of the asphalt binder should result in lower densities, increased voids and more random particle orientation, all of which combine to reduce the velocity of the mechanical wave. Asphalt contents above this "optimum" will tend to force the aggregate particles apart, reduce inter-particle contact and force the wave to travel through the acoustically slower asphalt cement for longer periods. This will increase the travel time of the wave and greatly reduce its velocity.

The contradiction between these results and those of the earlier study is believed to be related to the differences in the aggregate used in the two mix designs. Of particular significance is the difference in surface texture of the two aggregates. Since the aggregate constitutes approximately 90% of the volume of the mixture, the aggregate characteristics will have a large influence on the mechanical properties of the

asphalt concrete and, therefore, a large influence on the rate of wave transmission through the material. The interaction of the aggregate grains occurs primarily through inter-particle friction. The factors contributing to inter-particle friction are 1) particle surface texture, 2) particle shape, 3) void ratio, 4) particle size, and 5) particle gradation. The most important of these is, however, the surface texture of the particle. The aggregate used in the earlier study was a well-graded silicous river sand. The sand had rounded particles with a top size of three-eighths inch. In this study, a crushed limestone and two different sands were combined to also provide a well-graded material. The grains were angular and had a top size of one-half inch. Additional research in this area is needed before more definite conclusions can be drawn.

Void Content Effects

In an attempt to define the relationship between the percentage of voids in the test material to the velocity of an ultrasonic wave through it, fifteen specimens were compacted using the Hveem-gyratory technique. The void contents ranging from 0.84% to 11.22% by volume were obtained by varying the total compactive effort applied to the specimen. Compressional wave and shear wave velocity measurements were then made at -15°F and 80°F.

Compressional Wave Tests

Figure 34 shows a plot of compressional wave velocity versus void content. A considerable amount of data scattering is evident, although the difference between the maximum velocity and the minimum velocity was

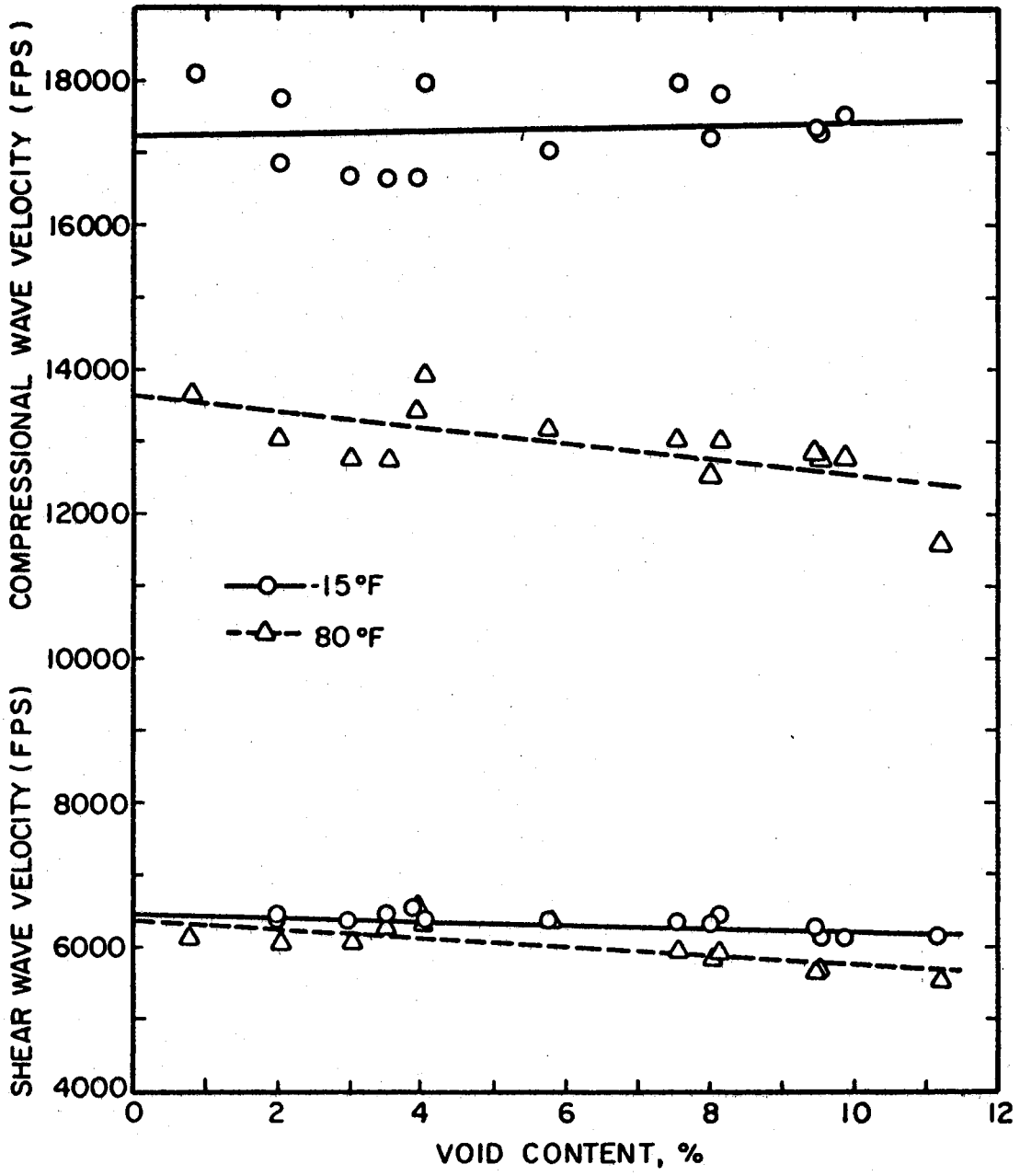

Figure 34. Effect of Per Cent Void Content on Ultrasonic Wave Velocity

only 1416 fps (8% of maximum) for the -15°F tests and 2360 fps (17% of maximum) for the 80°F tests. Due to the apparent linear relationship, linear regression lines were determined for these two data sets. The slope of the -15°F linear regression line was +15.20 (fps/% void content). The line is essentially horizontal indicating a negligible effect of voids contained in the test material on the wave velocity at that temperature. On the other hand, the slope of the 80°F linear regression line was -107.04 (fps/% void content). This indicates that an increase of the amount of voids in a specimen at 80°F caused a decrease in the rate of transmission of the compressional wave through the material.

Shear Wave Tests

Figure 34 also shows a plot of shear wave velocity versus per cent voids for tests at -15°F and 80°F.

These show the same general trend as did the compressional wave plots. The slope of the linear regression line for the -15°F test is -24.18 (fps/% void content), indicating a minor effect of void content on the velocity of the shear wave through the specimen. At laboratory temperature (80°F), the linear regression line slope (-62.19) indicates an increased dependency of shear wave velocity on the void content of the specimen, although not as great as does the compressional wave velocity.

The data scatter in both the compression and the shear tests are probably attributable to the fact that the size of the aggregate particles, as well as their orientation in the asphalt-aggregate matrix, have a large influence on the rate of transmission of an elastic wave through

the material. The aggregate used in the mix, as previously stated, had a top size of one-half inch. Orientation of several of these larger particles such that most of the travel path (±2.0 inches) of the elastic wave was through these particles would result in high velocities. The velocities of waves having travel paths through more of the asphalt cement rather than the aggregate constituent would have slower travel velocities.

Taking into account testing error and normal data scatter, Figure 34 reveals that the amount of voids in a material specimen at low temperature had little, if any, effect on the rate of transmission of the ultrasonic wave. The increased viscosity of the asphalt binder at these temperatures seems to be of primary influence. At the higher temperature, where the asphalt viscosity is less and the asphalt volume is greater, the amount of voids included in the matrix is relatively more important. This indicates that the nature of the binder has a smaller influence on inter-particle contact in the more dense specimens than in the less dense specimens. That is, the better aggregate-to-aggregate contact in the denser or more highly compacted material results in a relatively higher rate of transmission of the acoustic wave.

"Elastic" Constants

Admittedly, asphalt concrete can be thought of as an elastic material only under certain conditions. Primarily, these conditions are low material temperature, where the plastic properties of the matrix are reduced, and low magnitude of loading. The assumption of homogeneity, also necessary for elastic theory, can be made only in the generalization that the matrix is equally inhomogeneous in all

directions. However, most engineers are so familiar with such material parameters as Poisson's ratio (ν), Young's Modulus, and the Shear Modulus that there does seem to be some value in determining these or similar parameters from wave velocity measurements. Such values should characterize a material and its behavior under varying conditions as well as the more fundamental factors rooted in the classical theory of elasticity.

In recognition of the difference between Young's modulus for a homogeneous, elastic material such as steel and the stress-strain relationship for asphalt-aggregate material, various investigators have called this relationship the sonic modulus, modulus of resilient deformation, deformation modulus, E-modulus, etc., depending upon the type of test used to determine the value. Likewise, the shear modulus is often designated as simply the G-modulus. The assumption of elasticity, although not theoretically valid, does permit these quantities to be handled with some familiarity. The equations relating shear and compressional wave velocity to the "elastic" constants have been derived in the Appendix.

E-Modulus

A plot of E-modulus values versus temperature for the respective asphalt content mixtures is shown in Figure 35. E-modulus values ranged from a high of 5.03×10^6 psi for the 6% asphalt content specimens at -15°F to a low of 0.35×10^6 psi for the 8% asphalt content specimen at 160°F. The amount of decrease in the E-modulus values between -15°F and 160°F was in the range of 86%. The decrease in E-modulus with temperature was also an expected occurrence. Similar

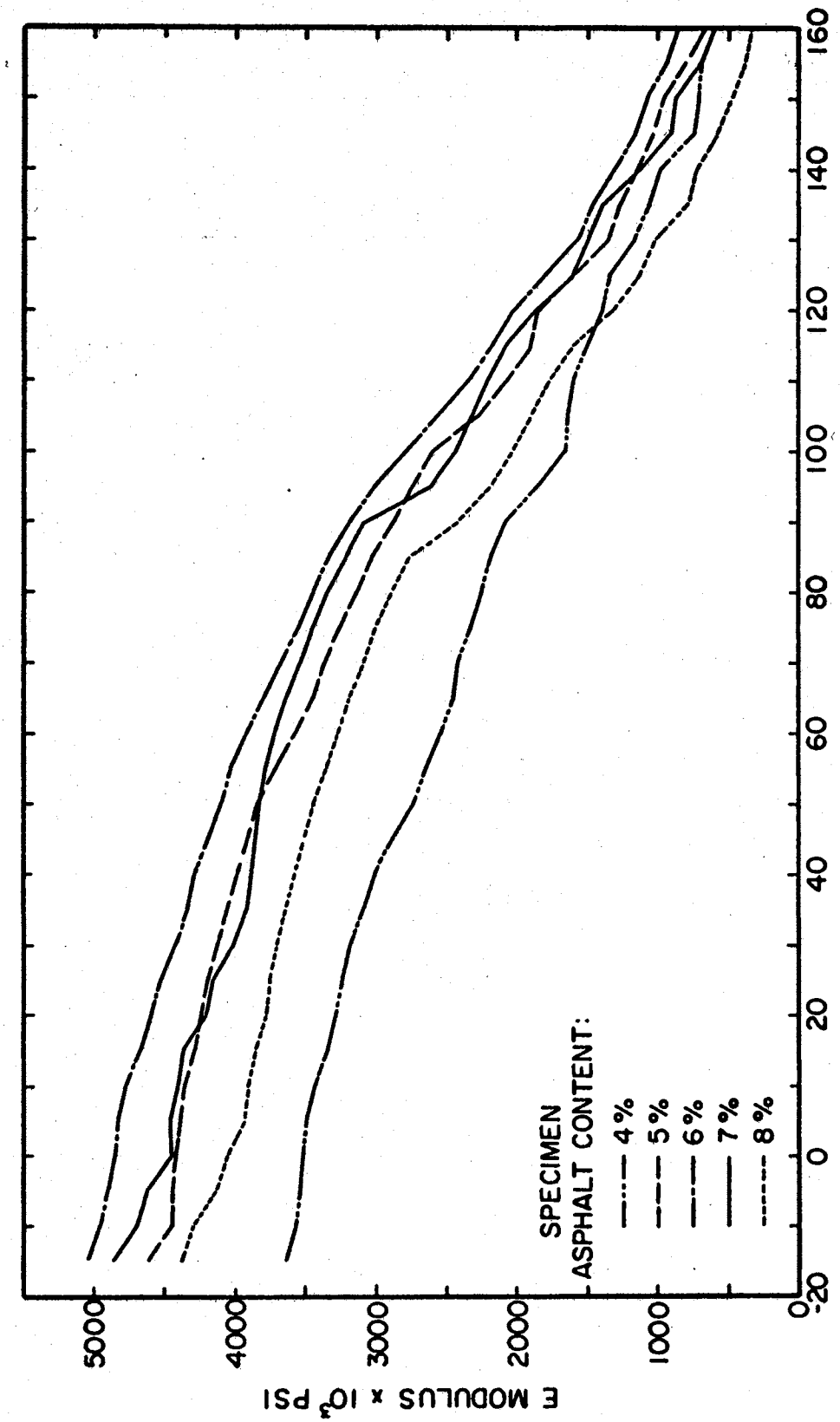

Figure 35. E-Modulus Versus Temperature

findings have been reported by Goetz (9), Kalles and Riley (22), as well as Kingham and Reseigh (23).

Various investigators have demonstrated the relationship of the so-called E-modulus to both the frequency of loading and the loading stress for asphalt concrete material (22) (36). They have shown that the E-modulus values vary directly with frequency and inversely with loading stress. The values of the E-modulus presented here are in excellent agreement with the sonic modulus values reported by Goetz (9). Monismith et al. (36), using repeated-load compression tests, reported values of the modulus of resilient deformation (E_e) in the range of 8×10^5 psi. Their tests used a deviator stress of 20-40 psi, however, much larger than that induced in the ultrasonic technique. Gregg et al. (10), utilizing a triaxial testing method with low frequency repetition, reported moduli of resilient deformation for bituminous stabilized sand bases in the range of 2.2×10^5 psi.

Since, in this procedure, E-modulus is determined from evaluation of the compressional and shear wave velocities, any factor influencing these velocities are mirrored in the E-moduli values. The plot indicates that the E-modulus is very significantly influenced by temperature and, to a lesser degree, by the asphalt content. E-modulus values increase with asphalt content up to 6%. Above this asphalt limit, the moduli decrease. Again, the maximum E-modulus seems to correlate with the asphalt content at which maximum wave transmission rate occurs. Since, in classical elastic theory, E is the ratio of applied stress to strain, it would indicate that those conditions that promote maximum wave velocity also result in the greatest stress-strain ratio for the material. The limiting factors, of course, are the assumption of

elasticity, the loading stress and rate of loading. Further investigation is needed, however, before a definite conclusion is made.

G-Modulus

The determination of the G-modulus of a material is an attempt to quantify the shear properties of the test material. In classical theory the shear modulus is the ratio of shear stress to shear strain. Again, the assumption of elastic behavior is made. Since the G-modulus is a function only of the shear wave velocity and mass density of the material (see Appendix), the relationship of G-modulus to temperature (Figure 36) is generally the same as for the shear wave velocity-temperature plot. The G-modulus values ranged from a maximum of 1.81×10^6 psi for the 6% asphalt content specimen at -15°F to 0.117×10^6 psi for the 8% asphalt content specimen at 160°F. The average decrease in G-modulus exhibited by the respective mixtures was approximately 87% of the maximum or low temperature modulus. As with the E-modulus plots, the G-modulus is a maximum throughout the temperature range for the 6% asphalt content mix.

Poisson's Ratio

Poisson's ratio, an elastic parameter, is the ratio of the unit lateral deformation to the unit longitudinal deformation of a specimen. This constant is often related to the "stiffness" of a material. Steel has a Poisson's ratio of approximately 0.30 while rubber has a Poisson's ratio of approximately 0.50.

Figure 37 is a plot of Poisson's ratio versus temperature for the 5% and the 8% specimens. The behavior is typical of the specimens at

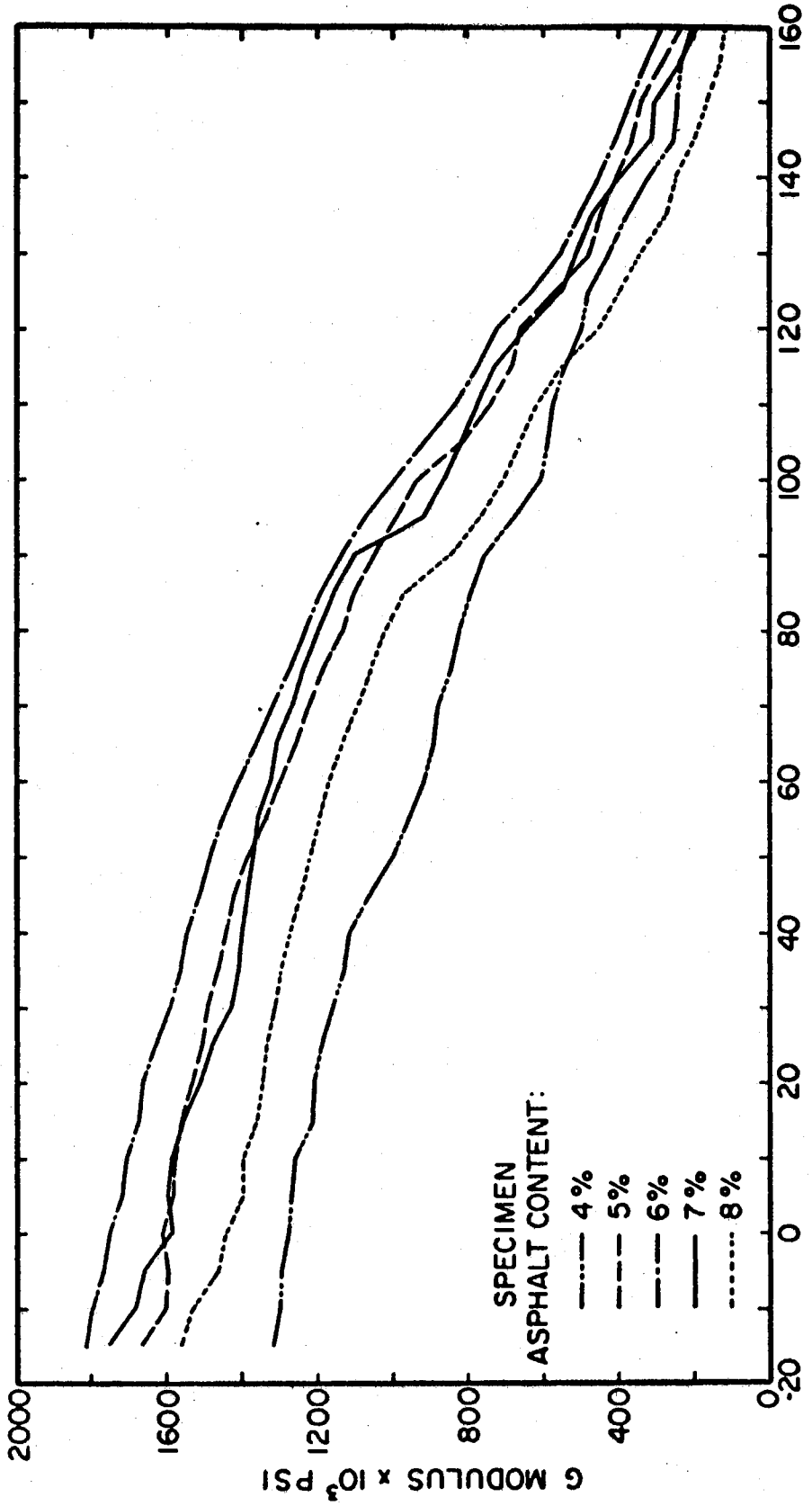

Figure 36. G-Modulus Versus Temperature

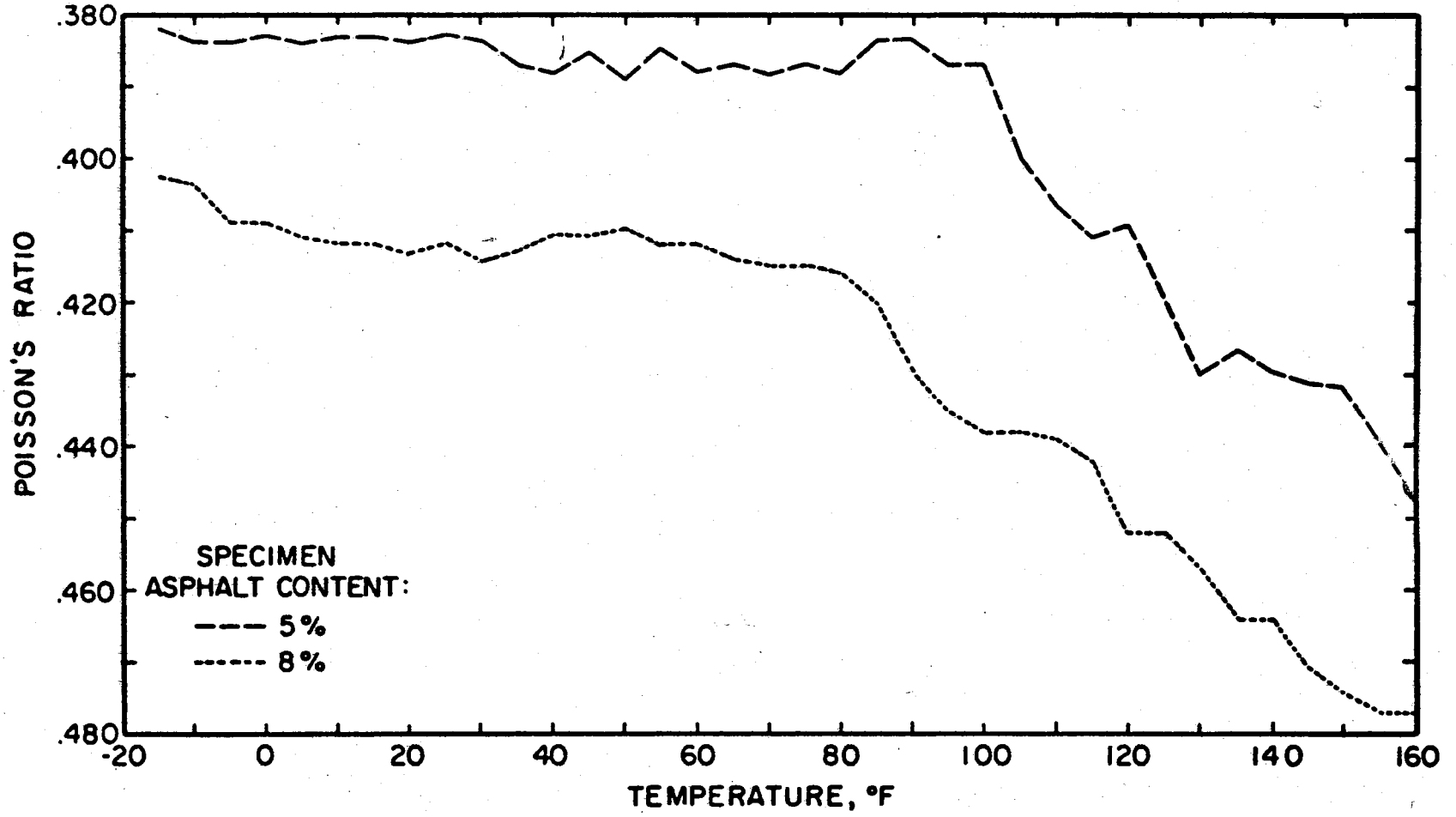

Figure 37. Poisson's Ratio Versus Temperature

other asphalt contents. The plot shows that at low temperatures, Poisson's ratio for the 5% specimen is approximately 0.385 while that for the 8% specimen is 0.405. Both values hold reasonably constant until a temperature of between 80°F and 100°F is reached. These values are in the same range as average values for silver (0.38), brass (0.374), lucite (0.40), and nylon (0.40), indicating the rigidity or stiffness of the asphalt concrete at these low and intermediate temperatures in the test range. Between 80°F and 100°F, Poisson's ratio for both specimens begins to increase rapidly until a value of 0.449 and 0.477 is reached at 160°F for the 5% and 8% asphalt content specimens, respectively. As would be expected, the ratios at the higher temperatures approach the theoretical maximum ratio of 0.50.

These plots also illustrate the effect of asphalt content on Poisson's ratio, i.e., Poisson's ratio increased monotonically with increasing asphalt content of the specimens. This further reflects the behavioral dependency of the material on the visco-elastic nature of the binder. When the test specimen was heated to the point at which the asphalt binder began to soften, the change in asphalt consistency caused a significant loss of rigidity in the material.

Tests on Marshall Specimens

In the latter stages of this investigation, an attempt was made to compare the elastic wave velocities exhibited by a series of specimens compacted by the Marshall method with those determined for the Hveem-Gyratory specimens. Although both shear and compressional velocities in the kneaded or gyratory compacted specimens were generally greater than in the specimens compacted by the impact procedure, not enough

information was available to provide conclusive results as to the effect of compaction method. However, the data developed from these tests indicate that the type of compaction method probably exerts an indirect influence on the wave velocity through a compacted specimen. This influence is no doubt related to the ultimate orientation of the aggregate particles.

CHAPTER VI

CONCLUSIONS

The primary objective of this study was to develop a technique to measure the velocity of an ultrasonic shear wave propagated through asphalt concrete. This technique, along with measurements of the ultrasonic longitudinal wave velocity, would provide a new nondestructive method for delineating the dynamic properties of asphalt-aggregate mixtures.

It can be concluded from the preliminary tests that it is indeed possible to measure ultrasonic shear wave velocities through standard size specimens of compacted asphalt-aggregate material. It has been demonstrated that the ultrasonic testing procedure developed in this paper can be used to yield beneficial information regarding the dynamic properties of asphalt concrete. This nondestructive testing procedure shows great promise of yielding useful information concerning the behavioral characteristics of other types of pavement construction materials as well. The possibility also exists that material parameters determined by this or similar techniques will have some application in the area of design, control, and subsequent in-situ evaluation of flexible pavement components.

A brief, non-statstical study of a single asphalt-aggregate mixture resulted in the following observations concerning the behavior of the material:

1. The temperature of the asphalt-aggregate test material had a great influence on the velocities of both the shear and compressional waves. Both velocities decreased with increasing temperature. The rate of decrease of the velocity increased with increasing temperature. The amplitudes of both wave types was a maximum at approximately 100°F. Wave attenuation increased as temperature varied above or below this optimum temperature.
2. Wave velocities were at a maximum in specimens compacted with asphalt contents between 6 and 7%. An increase above 7% or a decrease below 6% asphalt content resulted in reduced velocities. Thus, an "optimum" asphalt content for wave transmission existed at 6-7% asphalt.
3. At -15°F, the amount of voids contained in a compacted asphalt-aggregate specimen had no effect on either the compressional or shear wave velocity. At laboratory temperature (80°F), however, an increase in voids resulted in a decrease in wave velocity. This trend was most evident for the compressional wave.
4. The E-moduli and the G-moduli, calculated using the wave velocity measurements, decreased with increasing temperature. The rate of decrease also increased with increasing temperature. The maximum moduli were associated with the test specimens containing 6% asphalt cement.
5. Poisson's ratio increased monotonically with increasing asphalt content of the specimens. The values were essentially constant until a temperature between 80° and

100°F was reached. Beyond this limit, Poisson's ratio rapidly increased to approximately 0.50. This behavior is probably indicative of the influence of the viscous properties of the asphalt binder.

6. The type of compaction method used for asphalt-aggregate mixtures exerts some influence on the ultrasonic wave velocities. This effect is probably related to the ultimate particle orientation and effect of intergranular contact in the compacted specimens.
7. Thermistors, implanted in the test specimens, provided accurate and continuous monitoring of internal specimen temperature.

CHAPTER VII

RECOMMENDATIONS FOR FURTHER RESEARCH

This investigation has brought to light areas in which additional work is needed. It is suggested that further studies in this field should be directed in the following areas:

1. Further refinement of the instrumentation procedure is needed. Of first concern should be the improvement of the pulse generation technique. Special regard should be paid to the shortening of the time length of the pulse. The adaptation of high voltage pulse generators, now commercially available, could allow flexibility in pulse length, frequency variation, and internal damping. It should be possible, with certain improvements in equipment, to measure both longitudinal and transverse wave velocities simultaneously. A shearing mode transducer with a resonant frequency in the 100 kilohertz range, coupled with a buffer rod between the transducer and the test material, would allow distinct differentiation between compression and shear waves detected at the receiver. The problem of securing good coupling between the crystal/buffer and buffer/test material interfaces would have to be overcome, possibly through the use of wax or some type of cementing agent as a couplant material.

The use of larger diameter crystals would reduce the tendency of the input wave pattern to have a spherical wave front. This could eliminate some of the mode conversion tendencies, particularly those occurring at the edges of the specimen. The larger crystal area, however, would increase the possibility of faulty coupling of the crystal to the specimen. Because of the roughness of the test specimen surface, some type of protective coating on the crystal is needed to reduce erosion of the transducer surface.

2. Instrumentation and measurement techniques should be developed by which the attenuation of an ultrasonic wave traveling through asphalt concrete can be measured. It is possible that the attenuation, along with wave velocity, is directly related to various material properties. The 'sing around' technique for attenuation measurements, as described in Chapter III, shows promise for use with asphalt concrete materials.
3. Correlation of ultrasonic E and G-moduli to static E and G-moduli should be attempted. While no direct correlation may be possible, such a study should provide additional information regarding the value of the ultrasonically determined parameters.
4. A study relating the ultrasonic moduli values to the standard Marshall and Hveem stabilities would be worthwhile.
5. The effects of aggregate type, shape size, gradation and surface texture on the ultrasonic wave velocities

should be investigated.

6. Procedures should be evolved by which this method of test can be applied to the testing of in-situ pavement structures. The procedures would, of necessity, have to be effective with access available to only one side of the structure. This would dictate either a pulse echo technique or measurement of Rayleigh (surface) waves. Preliminary testing of specimens cored from existing pavements should give an indication of the applicability of the echo technique to the in-situ material.
7. Ultrasonic wave velocity measurements should be applied to the investigation of soils. This testing technique shows promise of being an efficient means of quantifying various dynamic soil properties nondestructively.

BIBLIOGRAPHY

(1) Akashi, Tyoki. "On the Measurement of Velocity and Loss of Ultrasonic Pulse in Concrete." Ultrasonic Testing. London: Butterworths Sci., 1964.

(2) Akroyd, T. N. W., and R. Jones. "Non-Destructive Testing of Structural Concrete by the Ultrasonic Pulse Technique." Proceedings, 4th International Conference on Non-Destructive Testing. London, 1963. London: Butterworths Sci., 1964.

(3) Brown, Stephen F., and Peter S. Pell. "Subgrade Stress and Deformation Under Dynamic Load." Journal of the Soil Mechanics and Foundations Division, ASCE, Vol. 93, No. SM1, Proc. Paper 5057 (January, 1967).

(4) Burchett, James O'Neill. "Time Domain Reflectometry for Measuring Viscoelastic Properties." (Unpub. Ph.D. dissertation, Oklahoma State University, May, 1966.)

(5) Chen, Hsing Huan, and Robert G. Hennes. "Dynamic Design of Bituminous Pavements." The Trend in Engineering (January, 1950), pp. 22-25.

(6) Dunegan, H. L. "High Temperature Dynamic Modulus Measurements by Use of Ultrasonics." Materials Evaluation, Vol. 22, No. 6 (1964), p. 266.

(7) Erlenbach, L. "The Usage of Dynamic Testing of Foundations." Published by the Deutsches Gesellschaft fur Bodenmechanik (DEGEBO), 1933.

(8) Filipczynski, L., Z. Pawlowski, and J. Wehr. Ultrasonic Methods of Testing Materials. London: Butterworth, 1966.

(9) Goetz, W. H. "Sonic Testing of Bituminous Mixtures." Proceedings, Association of Asphalt Paving Technologists, Vol. 24 (1955), pp. 332-348.

(10) Gregg, J. S., G. L. Dehlen, and P. J. Rigden. "On the Properties, Behavior and Design of Bituminous Stabilized Sand Bases." Proceedings, Second International Conference on the Structural Design of Asphalt Pavements, August 7-11, 1967, Ann Arbor, Michigan.

(11) Hampton, Loyd D. "Acoustic Properties of Sediments." The Journal of the Acoustical Society of America, Vol. 42, No. 4 (June, 1967), pp. 882-890.

(12) Hertwig, A., A. Fruh, and H. Lorenz. "The Usage of Vibrational Techniques to Determine the Properties of Soil Important to Structural Work." Published by the Deutsches Gesellschaft fur Bodenmechanik (DEGEBO), 1933.

(13) Heukelom, W., and T. W. Niesman. "Method of Investigation and Apparatus Used by the Koninlijke/Shell Laboratorium, Amsterdam, Holland."

(14) Heukelom, W. "Dynamic Testing of Pavements: Survey of Theoretical Considerations." Koninklijke/Shell Laboratorium, Amsterdam, Holland.

(15) Heukelom, W., and A. J. G. Klomp. "Dynamic Testing as a Means of Controlling Pavements During and After Construction." Proceedings, International Conference on the Structural Design of Asphalt Pavements, August 20-24, 1962. Ann Arbor, Michigan, pp. 667-679.

(16) Iwatake, M., and T. Takabayashi. "Nondestructive Testing on Concrete Pavements by Ultrasonic Wave." Ultrasonic Testing. London: Butterworths Sci., 1964.

(17) Jaffe, Bernard. "A Primer on Ferroelectricity and Piezoelectric Ceramics." Technical Paper TP-217, Electronic Research Division, Clevite Corp., Eng. Memo #60-14, Dec., 1960.

(18) Jaffe, Hans. "Piezoelectricity." Encyclopedia Britannica, 1961.

(19) Jimenez, Rudolf, A., and Bob M. Gallaway. "Behavior of Asphaltic Concrete Diaphragms to Repetitive Loadings." Proceedings, International Conference on the Structural Design of Asphalt Pavements, August 20-24, 1962. Ann Arbor, Michigan, pp. 339-344.

(20) Jones, R. "Following Changes in the Properties Road Bases and Sub-Bases by the Surface Wave Propagation Method." Civil Engineering and Public Works Review, 1963, 58 (682) 777-80 May and June, 1963.

(21) Jones, R. "The Ultrasonic Testing of Concrete." Ultrasonics, Vol. 1 (1963).

(22) Kallas, B. F., and J. C. Riley. "Mechanical Properties of Asphalt Pavement Materials." Proceedings, Second International Conference on the Structural Design of Asphalt Pavements, August 7-11, 1967, Ann Arbor, Michigan.

(23) Kingham, R. Ian, and T. C. Reseigh. "A Field Study of Asphalt-Treated Bases in Colorado." Proceedings, Second International Conference on the Structural Design of Asphalt Pavements, August 7-11, 1967, Ann Arbor, Michigan.

(24) Kolsky, H. Stress Waves in Solids. New York: Dover Publications, Inc., 1963.

(25) Krautkramer, J., and H. Krautkramer. Ultrasonic Testing of Materials. New York: Springer-Verlong, Inc., 1969.

(26) Krokosky, J. P. Chen. "Viscoelastic Analysis of the Marshall Test." Presented at the 39th Annual Meeting of the Association of Asphalt Paving Technologists, Dallas, Texas, February, 1964.

(27) Lee, Kenneth L., and H. Bolton Seed. "Dynamic Strength of Anisotropically Consolidated Sand." Journal of the Soil Mechanics and Foundation Division, ASCE, Vol. 93, No. SM5, Proc. Paper 5451, (September, 1967), pp. 1969-190.

(28) Levitt, A., P., and A. G. Martin. "Ultrasonic Determination of Elastic Constants, of Metals at Elevated Temperatures." Nondestructive Testing, Vol. 18 (1960), pp. 333-336.

(29) McGonnagle, W. J. "Ultrasonic Shear Wave Testing." Metal Progress (October, 1956).

(30) McSkimin, H. J. "Ultrasonic Measurement Technique Applicable to Small Solid Specimens." Journal of the Acoustical Society of America, Vol. 22 (1950), pp. 413.

(31) _____. "Propagation of Longitudinal Waves and Shear Waves in Cylindrical Rods at High Frequencies." Journal of the Acoustical Society of America, Vol. 28 (1956), pp. 484.

(32) Manke, P. G., and B. M. Gallaway. "Pulse Velocities in Flexible Pavement Construction Materials." A paper presented to the Highway Research Board, Washington, D. C., January 17-21, 1966.

(33) Mason, W. P., and H. J. McSkimin. "Attenuation and Scattering of High Frequency Sound Waves in Metals and Glasses." Journal of the Acoustical Society of America, Vol. 19 (1947), pp. 464.

(34) Metcalf, C. T. "Field Measurement of Dynamic Elastic Moduli of Materials in Flexible Pavement Structures." Proceedings, Second International Conference on the Structural Design of Asphalt Pavements, August 7-11, 1967, Ann Arbor, Michigan.

(35) Monismith, Carl L. "Effect of Temperature on the Flexibility Characteristics of Asphaltic Paving Mixtures." Presented to the Third Pacific Area National Meeting of the American Society for Testing Materials, San Francisco, Calif. (1959).

(36) Monismith, C. L., R. L. Terrel, and C. K. Chan. "Load Transmission Characteristics of Asphalt-Treated Base Courses." Proceedings, Second International Conference on the Structural Design of Asphalt Pavements, August 7-11, 1967, Ann Arbor, Michigan.

(37) Nijboer, L. W., and C. Van Der Poel. "A Study of Vibration Phenomena in Asphaltic Road Construction." Proceedings, Association of Asphalt Paving Technologists, 22: 197-231. Discussion, 232-277 (1953).

(38) Pagen, Charles A. "A Study of the Temperature-Dependent Rheological Characteristics of Asphaltic Concrete." Presented at the Annual Meeting of the Highway Research Board, Washington, D. C., January 17-21, 1966.

(39) Papazian, Hratch S. "The Response of Linear Viscoelastic Materials in the Frequency Domain With Emphasis on Asphalt Concrete." Proceedings, International Conference on the Structural Design of Asphalt Pavements, August 20-24, 1962, Ann Arbor, Michigan, pp. 454-463.

(40) Parker, W. E. "Pulse Velocity Testing of Concrete." Proceedings, American Society for Testing Materials, Vol. 53 (1953).

(41) Ramspeck, A., and C. A. Schulze. "The Dispersion of Elastic Waves in Soils." Published by the Deutsches Gesellschaft fur Bodenmechanik (DEGEBO), 1938.

(42) Redwood, M. "Ultrasonic Waveguides - A Physical Approach." Ultrasonics (April-June, 1963), pp. 99-105.

(43) Sen-Gupta, B. K. "A Note on the Ultrasonic Pulse Technique for the Testing of Bricks." Civil Engineering and Public Works Review, Vol. 59, No. 691 (1964), p. 188.

(44) Shannon, William L., George Yamane, and Rudy J. Dietrich. "Dynamic Triaxial Tests on Sand." Presented at the 42nd Annual Meeting of the Highway Research Board, Washington, D. C., January, 1963.

(45) Sheeran, Donald E., Wallace H. Baker, and Raymond J. Krized. "Experimental Study of Pulse Velocities in Compacted Soils." Presented at the Forty-Sixth Annual Meeting of the Highway Research Board, Washington, D. C., January, 1967.

(46) Stephenson, Richard W. "Temperature Effects on the Compressional Wave Velocities of Asphalt-Aggregate Mixtures." (Unpub. M.S. thesis, Oklahoma State University, July, 1968.)

(47) Szendrei, Michael E., and Charles R. Freeme. "Road Responses to Vibration Tests." Journal of the Soil Mechanics and Foundations Division, ASCE, Vol. 96, No. SM6, Proc. Paper 7709 (November, 1970), pp. 2099-2124.

(48) Thrower, E. N. "Technique for Measuring the Elastic Properties of Bitumens, Tars, and Soils Under Dynamic Loading." J. Scientific Instruments, 38, (3) (1961), pp. 69-73.

(49) Truell, Rohn, Charles Elbaum, and Bruce B. Chick. Ultrasonic Methods in Solid State Physics. New York: Academic Press, 1969.

(50) Van Der Poel, C. "Dynamic Testing of Road Construction." Journal of Applied Chemistry, 1:7.

(51) Weissmann, Gerd F. "Vibrator for Soil Testing." Journal of the Soil Mechanics and Foundation Division, ASCE, Vol. 97, No. SM3 (Mar., 1971), pp. 601-605.

(52) Whiffin, A. C. "The Application of Elastic Theory to Flexible Pavements." Proceedings, International Conference on the Structural Design of Asphalt Pavements, August 20-24, 1962, Ann Arbor, Michigan.

(53) Whitehurst, E. A. "Soniscope Tests Concrete Structures." Journal of the American Concrete Institute, Proceedings Vol. 47 (February, 1951), p. 433.

(54) Standard Specifications for Highway Construction. Oklahoma State Highway Department, 708.01 (1967), p. 456.

(55) Kornilovich, Yu. E., and V. I. Belokhuustikova. Ultrasound in the Production and Inspection of Concrete, authorized translation from the Russian by James S. Wood, Consultants Bureau, New York, 1965.

APPENDIX

DERIVATION OF WAVE VELOCITY EQUATIONS

The theory of propagation of stress waves is developed from elastic theory. The variation in stress across a small elastic parallelepiped is shown in Figure 38. The forces acting on each face are proportional to the stresses at the center of the face multiplied by the area of the face. Looking at the force in the x direction:

$$F_x = (\sigma_{xx} + \frac{\partial \sigma_{xx}}{\partial x}\,\delta_x)\delta_y\delta_z - \sigma_{xx}\delta_y\delta_z + (\sigma_{xy} + \frac{\partial \sigma_{xy}}{\partial y}\,\delta y)\delta_x\delta_z - \sigma_{xy}\delta_x\delta_z +$$

$$+ (\sigma_{xz} + \frac{\partial \sigma_{xz}}{\partial z}\,\delta_z)\delta_x\delta_y - \sigma_{xz}\delta_x\delta_y \qquad (1)$$

simplifying:

$$F_x = \left(\frac{\partial \sigma_{xx}}{\partial x} + \frac{\partial \sigma_{xy}}{\partial y} + \frac{\partial \sigma_{xz}}{\partial z}\right)\delta_x\delta_y\delta_z . \qquad (2)$$

Neglecting body forces, Newton's second law of motion states that the sum of the forces in a given direction is equal to the mass of the particle times the acceleration in that direction; i.e.:

$$F_x = \left[(\rho\,\delta_x\,\delta_y\,\delta_z)\,\frac{\partial^2 u}{\partial t^2}\right] \qquad (3)$$

where:

ρ = density = $\frac{\gamma}{g}$

u = displacement in x direction

γ = bulk density

g = acceleration due to gravity.

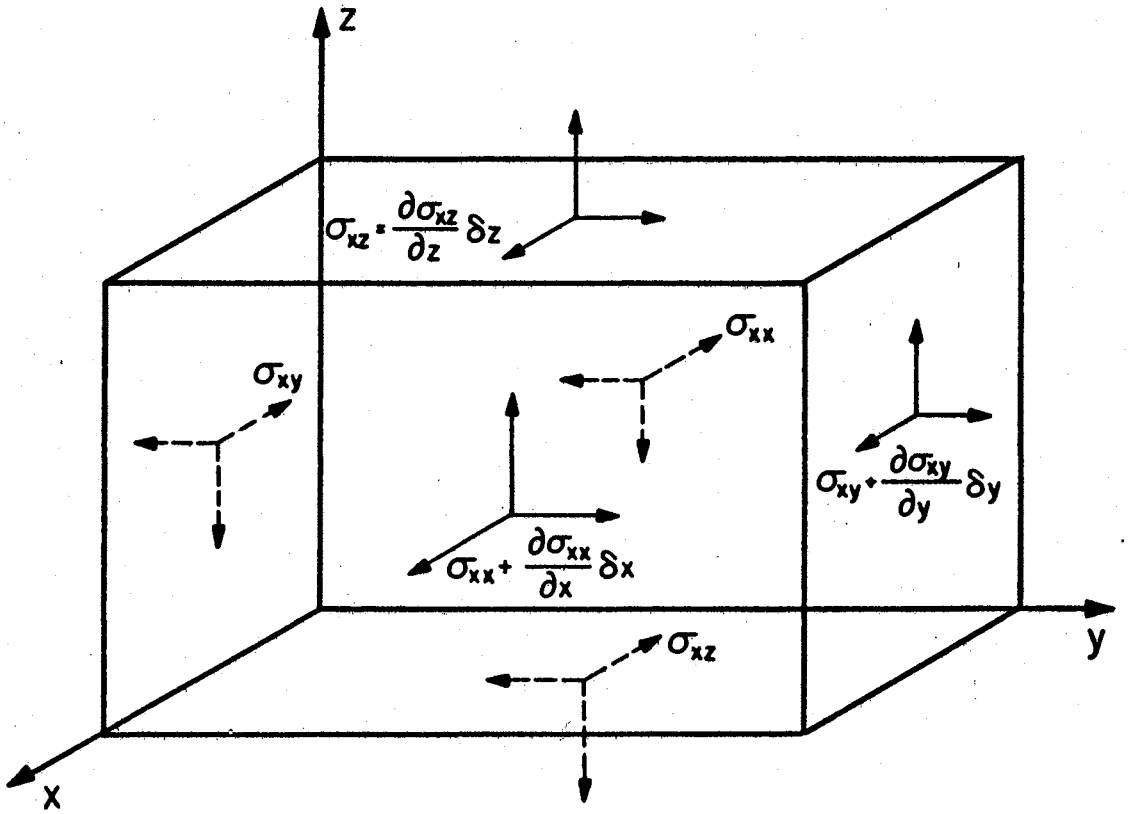

Figure 38. Stresses Acting in X-Direction On a Small Rectangular Parallelepiped

Therefore:

$$\rho \frac{\partial^2 u}{\partial t^2} = \frac{\partial \sigma_{xx}}{\partial x} + \frac{\partial \sigma_{xy}}{\partial y} + \frac{\partial \sigma_{xz}}{\partial z} \tag{4a}$$

$$\rho \frac{\partial^2 v}{\partial t^2} = \frac{\partial \sigma_{yx}}{\partial x} + \frac{\partial \sigma_{yy}}{\partial y} + \frac{\partial \sigma_{yz}}{\partial z} \tag{4b}$$

$$\rho \frac{\partial^2 w}{\partial t^2} = \frac{\partial \sigma_{zx}}{\partial x} + \frac{\partial \sigma_{zy}}{\partial y} + \frac{\partial \sigma_{zz}}{\partial z} \tag{4c}$$

where:

v = displacement in y direction

w = displacement in z direction.

Hooke's law states that each of the components of stress is at any point a linear function of the six components of strain. In general:

$$\sigma_{xx} = c_{11}\epsilon_{xx} + c_{12}\epsilon_{yy} + c_{13}\epsilon_{zz} + c_{14}\epsilon_{yz} + c_{15}\epsilon_{zx} + c_{16}\epsilon_{xy} \tag{5a}$$

$$\sigma_{yy} = c_{21}\epsilon_{xx} + c_{22}\epsilon_{yy} + c_{23}\epsilon_{zz} + c_{24}\epsilon_{yz} + c_{25}\epsilon_{zx} + c_{26}\epsilon_{xy} \tag{5b}$$

$$\sigma_{zz} = c_{31}\epsilon_{xx} + c_{32}\epsilon_{yy} + c_{33}\epsilon_{zz} + c_{34}\epsilon_{yz} + c_{35}\epsilon_{zx} + c_{36}\epsilon_{xy} \tag{5c}$$

$$\sigma_{yz} = c_{41}\epsilon_{xx} + c_{42}\epsilon_{yy} + c_{43}\epsilon_{zz} + c_{44}\epsilon_{yz} + c_{45}\epsilon_{zx} + c_{46}\epsilon_{xy} \tag{5d}$$

$$\sigma_{zx} = c_{51}\epsilon_{xx} + c_{52}\epsilon_{yy} + c_{53}\epsilon_{zz} + c_{54}\epsilon_{yz} + c_{55}\epsilon_{zx} + c_{56}\epsilon_{xy} \tag{5e}$$

$$\sigma_{xy} = c_{61}\epsilon_{xx} + c_{62}\epsilon_{yy} + c_{63}\epsilon_{zz} + c_{64}\epsilon_{yz} + c_{65}\epsilon_{zx} + c_{66}\epsilon_{xy}. \tag{5f}$$

In order to satisfy the condition that the elastic energy be a univalued function of the strain, any coefficient c_{rs} must be equal to the coefficient c_{sr}. In an isotropic solid, the values of the coefficients must be independent of the rectangular axis system chosen and, therefore, only two independent constants remain, λ and μ (Lame's constants).

$$c_{12} = c_{13} = c_{21} = c_{23} = c_{31} = c_{32} = \lambda \tag{6a}$$

$$c_{44} = c_{55} = c_{66} = \mu \tag{6b}$$

$$c_{11} = c_{22} = c_{33} = \lambda + 2\mu. \tag{6c}$$

All the other constants are zero.

Therefore, Equations (5) become:

$$\sigma_{xx} = \lambda\Delta + 2\mu\epsilon_{xx} \tag{7a}$$

$$\sigma_{yy} = \lambda\Delta + 2\mu\epsilon_{yy} \tag{7b}$$

$$\sigma_{zz} = \lambda\Delta + 2\mu\epsilon_{zz} \tag{7c}$$

$$\sigma_{yz} = \mu\epsilon_{yz} \tag{7d}$$

$$\sigma_{zx} = \mu\epsilon_{zx} \tag{7e}$$

$$\sigma_{xy} = \mu\epsilon_{xy} \tag{7f}$$

where:

$$\Delta = \epsilon_{xx} + \epsilon_{yy} + \epsilon_{zz}.$$

Now, From Equations (4a-c), using Equations (7a-f):

$$\rho\frac{\partial^2 u}{\partial t^2} = \frac{\partial}{\partial x}(\lambda\Delta + 2\mu\epsilon_{xx}) + \frac{\partial}{\partial y}(\mu\epsilon_{xy}) + \frac{\partial}{\partial z}(\mu\epsilon_{xz}). \tag{8}$$

Since:

$$\epsilon_{xx} = \frac{\partial u}{\partial x}\ ;\ \epsilon_{xz} = \frac{\partial w}{\partial x} + \frac{\partial u}{\partial z}\ ;\ \epsilon_{xy} = \frac{\partial v}{\partial x} + \frac{\partial u}{\partial y}$$

$$\rho\left(\frac{\partial^2 u}{\partial t^2}\right) = (\lambda + \mu)\frac{\partial\Delta}{\partial x} + \mu\,\nabla^2 u \tag{9}$$

$$\rho\left(\frac{\partial^2 v}{\partial t^2}\right) = (\lambda + \mu)\frac{\partial \Delta}{\partial y} + \mu \nabla^2 v \qquad (10)$$

$$\rho\left(\frac{\partial^2 w}{\partial t^2}\right) = (\lambda + \mu)\frac{\partial \Delta}{\partial z} + \mu \nabla^2 w \qquad (11)$$

where

$$\nabla^2 = \left(\frac{\partial^2}{\partial x^2} + \frac{\partial^2}{\partial y^2} + \frac{\partial^2}{\partial z^2}\right).$$

Differentiating Equation (9) with respect to x, Equation (10) with respect to y and Equation (11) with respect to z and adding:

$$\rho \frac{\partial^2 \Delta}{\partial t^2} = (\lambda + 2\mu) \nabla^2 \Delta$$

which is analogous to the wave form:

$$\frac{\partial^2 y}{\partial t^2} = c^2 \frac{\partial^2 y}{\partial x^2}.$$

This shows that the dilation Δ is propagated through the medium with a velocity $[(\lambda + 2\mu)/\rho]^{1/2}$. If, however, Δ is eliminated between Equations (10) and (11) by differentiating Equation (10) with respect to z and Equation (11) with respect to y and subtracting:

$$\rho \frac{\partial^2}{\partial t^2}\left(\frac{\partial w}{\partial y} - \frac{\partial v}{\partial z}\right) = \mu \nabla^2\left(\frac{\partial w}{\partial y} - \frac{\partial v}{\partial z}\right)$$

$$\rho \frac{\partial^2 \bar{w}_x}{\partial t^2} = \mu \nabla^2 \bar{w}_x$$

$\bar{w}_x$ is the rotation about the x axis.

Therefore:

$$\rho \frac{\partial^2 y}{\partial t^2} = \mu \nabla^2 u .$$

Therefore, waves with two differing velocities may be transmitted. Those with no rotation travel with $V = [(\lambda + 2\mu)/\rho]^{1/2}$ (compressional wave) and waves that travel with no dilation have a velocity $V = (\mu/\rho)^{1/2}$ (shear).

Hence:

$$V_c = \sqrt{\frac{\lambda + 2\mu}{\rho}}$$

and:

$$V_s = \sqrt{\frac{\mu}{\rho}}.$$

Since:

$$\lambda = \frac{\nu E}{(1+\nu)(1-2\nu)} \quad \text{and} \quad \mu = G = \frac{E}{2(1+\nu)}$$

ν = Poisson's ratio

$$V_c = \sqrt{\frac{E(1-\nu)}{\rho(1+\nu)(1-2\nu)}} \tag{12}$$

$$V_s = \sqrt{\frac{E}{2\rho(1+\nu)}} = \sqrt{\frac{G}{\rho}}. \tag{13}$$

Solving Equation (12) and (13) for G and E yields:

$$G = \rho V_s^2 \tag{14}$$

$$E = \left[3 - \frac{1}{\left(\frac{V_c}{V_s}\right)^2 - 1}\right] \rho V_s^2 \tag{15}$$

and

$$\nu = \frac{1 - \frac{1}{2}\left(\frac{V_c}{V_s}\right)^2}{1 - (V_c/V_s)^2}. \tag{16}$$

VITA

Richard Wesley Stephenson

Candidate for the Degree of

Doctor of Philosophy

Thesis: ULTRASONIC TESTING OF ASPHALT-AGGREGATE MIXTURES

Major Field: Engineering

Biographical:

Personal Data: Born in Tulsa, Tulsa County, Oklahoma, July 21, 1944, the son of F. W. and Hazel F. Stephenson.

Education: Attended elementary school in Tulsa, Oklahoma; graduated from Tulsa Thomas A. Edison High School in 1962; received the Bachelor of Science degree in Civil Engineering from the Oklahoma State University in July, 1967; received the Master of Science degree in Civil Engineering from the Oklahoma State University in July, 1968; completed requirements for the Doctor of Philosophy degree in Civil Engineering in May, 1972.

Professional Experience: Engineering Aide with Tulsa District, U. S. Corps of Engineers as hydrologic technician during summer, 1963; Engineering Aide with Tulsa District, U. S. Corps of Engineers as highway design technician, summer, 1964 and 1965; Highway Engineering Technician with the Alaska State Highway Department, Anchorage, Alaska, summer, 1966; Asphalt Materials Laboratory Assistant, Oklahoma State University, 1967; Engineering Aide with Tulsa District, U. S. Corps of Engineers as soils laboratory technician, summer, 1967; Research Assistant, Elastic Properties of Asphalt Materials Research Project, Oklahoma State University, Stillwater, Oklahoma, 1967-1969; Teaching Assistant in Engineering Mechanics, Oklahoma State University, Stillwater, Oklahoma, 1970-1971.